

DETERMINATION OF NITROGEN AND SULPHUR FUNCTIONALITY IN COAL AND COAL LIQUIDS

Stephen Wallace, Keith D. Bartle, Mark Baxby, Norman Taylor,
School of Chemistry, University of Leeds, Leeds, LS2 9JT, U.K.

Bernard B. Majchrowicz, J. Yperman, H.J. Martens, J. Gelan.
Department of Chemistry, Limburg University, B-3610 Diepenbeek,
Belgium.

INTRODUCTION

The type and distribution of nitrogen and sulphur functional groups in raw coal and their fate during processing have vital implications for the environmental impact of coal utilisation, as well as for the mechanism of the processes themselves. The combustion of nitrogen and sulphur rich fuels is known to release many hetero-PAC's, NO, and SO_x compounds into the atmosphere. NO and SO_x can be formed from the oxidation of nitrogen and sulphur compounds present in the fuel and, in the case of NO_x, also from atmospheric nitrogen (thermal NO_x). Whilst conventional petroleum derived fuels contain low enough heteroatom concentrations for thermal NO_x to predominate, in typical liquid fuels derived from coal, which have much higher heteroatom contents, fuel derived NO_x and SO_x are dominant¹. Furthermore, combustion of fuel bound nitrogen under fuel rich conditions can lead to the formation of HCN and NH₃, as well as NO_x.

The ultimate fate of the nitrogen and sulphur functional groups in coals and coal derived liquids is, however, dependent on the types of functional groups in which they are present. Non-basic nitrogen functions are thought to be the major source of NO_x emissions during combustion whilst reactive sulphur compounds, such as mercaptans, cause excessive metal corrosion during processing. In addition, some nitrogen and sulphur compounds (e.g. nitrogen bases) are known to reduce the useful lifetime of the catalysts used during the refining processes².

In this paper we report on methods which allow the analysis of nitrogen and sulphur functional groups in samples ranging from raw coals to process derived liquids and solids. X-ray photoelectron spectroscopy (XPS) has been combined with potentiometric titration and infra-red spectroscopy to provide a self consistent quantitative analysis of nitrogen functionality. Sulphur functional group distributions have been determined by temperature programmed reduction (TPR) and the method has been applied to study the hydrogen donor liquefaction of coal. The potential of using XPS as a method for the study of sulphur functional groups is also discussed.

EXPERIMENTAL

1) Materials

Two SRC process solvent residues (A, 397 °C; B, 351 °C), a coal liquid produced in a tubing bomb shaking autoclave from Burning Star coal, a Belgian (Beringen) coal and its SRC product were

studied. To facilitate nitrogen functional group determination, the samples were separated into n-pentane soluble, asphaltene and preasphaltene fractions³. The asphaltenes were further separated by a fractionation scheme outlined elsewhere^{4,5}. The scheme produced three nitrogen-rich fractions consisting of strong bases, weak bases (as quaternary salts) and neutrals. The fractions were then analysed by the methods outlined below.

2) X-Ray photoelectron spectroscopy

Photoelectron spectra were recorded on a Kratos ES300 spectrometer using AlK_α radiation. The spectrometer was run in fixed analyser transmission mode at a pass energy of 65eV, slit width 1.75 mm with an X-ray source power of 300 W. Powdered samples were mounted by pressing onto double sided adhesive tape and introduced into the spectrometer via a rapid insertion probe. Coal samples were ground under heptane in a ball mill to < 5µm and stored under heptane before use to minimise the effects of surface oxidation. Spectra were recorded at a pressure of less than 1×10^{-5} Pa. Data acquisition was controlled by a Kratos DS300 data system which was also used for spectral quantification and analysis. In order to obtain N(1s) spectra of sufficient quality to permit resolution of the different nitrogen components, long data acquisition times were required. For samples of the lowest nitrogen concentration this amounted to several hours of data accumulation. The nitrogen peak was resolved using a peak synthesis routine employing symmetric components of Gaussian line shape at fixed binding energies determined from model compound studies⁵. The intensities of the components were varied in order to obtain the best fit to the experimental spectrum while constraining the full widths at half maximum of all the components to be within the limits 1.8 to 2.0eV.

3) Infra-Red Spectroscopy

Quantitative infra-red spectra were recorded to determine the amount of nitrogen present as non-basic N-H. Spectra were recorded on a Perkin Elmer 1750 Fourier Transform Infra-red Spectrometer. Samples were dissolved in deuteriochloroform at low concentration (<30mg/10ml), to reduce hydrogen bonding, and spectra recorded in a 1 cm quartz cell.

Quantification of the N-H stretch ($3460-3480 \text{ cm}^{-1}$), for fossil fuel derived samples, was achieved from a calibration graph of absorbance at this wavelength versus NH concentration determined, by XPS. In all cases samples were methylated using diazomethane⁷ before analysis to remove the interfering OH absorptions.

4) Potentiometric Titration

Non-aqueous potentiometric titration was used to determine the basic nitrogen content of soluble samples⁶, including those samples of low molecular mass which were not amenable to study by XPS because of higher vapour pressure. Between 100mg and 500mg (depending on nitrogen content) of the sample was dissolved in a small quantity of benzene or chloroform before the addition of 50-75cm³ of the titration medium, glacial acetic acid. The titrant, 0.05M perchloric acid in glacial acetic acid, was added

via an automatic titration system and the end point detected using a combined glass and a calomel electrode.

5) Temperature Programmed Reduction

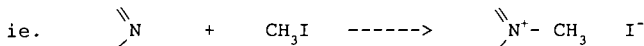
Temperature programmed reduction experiments were performed in a 3ml stainless steel reactor designed to give optimum recovery of sulphur. The samples (between 5mg and 75mg depending on sulphur content) were mixed with a reducing solvent mixture (phenanthrene, resorcinol, 9,10 dihydrophenanthrene, tetralin and pyrogallol) in the reaction vessel and sonicated for one hour. The reduction experiment was performed by fitting the reaction vessel to a stainless steel condenser arrangement and applying a temperature ramp of 7 °C/min to the cell. Any H₂S evolved was flushed from the cell by a stream of preheated nitrogen (30 ml/min) and make-up nitrogen was added (30 ml/min) to the gas stream immediately following the condenser system. The H₂S was detected by measuring the sulphide ion in an alkaline sulphur antioxidant buffer (SAOB) using a sulphur-specific electrode system. The sulphide electrode was calibrated by adding small amounts of sodium sulphide to the SOAB solution via an automatic burette. The electrode response was checked at the beginning and end of each run by adding a known concentration of sodium sulphide. Changes in the cell potential and reactor temperature were recorded by a computer data capture system and the data were subsequently output as plots of sulphur concentration versus temperature or as the integrated signal.

RESULTS AND DISCUSSION

1) Quantification of Nitrogen Functional groups

i) XPS of Nitrogen Containing Functional Groups

Table I shows the ultimate analysis data for the coal and coal derived products studied. In every case these products gave rise to a single, broad, N(1s) peak in their XPS spectra. In all cases, except for the quaternarised samples, the N(1s) spectra could be resolved into two major components at binding energies of 400.2eV and 398.8eV corresponding to nitrogen in pyrrole and pyridine type structures respectively⁵. The proportions of the two components were calculated for each fraction and are shown in Table I. The XPS spectra of the fractions quaternarised with methyl iodide are more complex since the reaction produces a pyridinium ion



This produces a shift in the pyridine N(1s) binding energy from 398.8eV to 401.4eV and the associated iodine concentration provides a further quantification of the pyridine groups. Since the pyridinium ion is unstable in the X-ray beam, however, the N(1s) spectrum consists of four components. From model compound studies using quaternarised phenanthridine, these were found to be, in order of decreasing binding energy, the quaternary salt

(401.4eV), pyrrole types (400.2eV), the degradation peak (399.5eV), and a small component due to residual pyridine types. The peak synthesis is simplified, however, because the quaternary and degradation product peaks are coupled and their ratios may be determined by analysis of the I(3d_{5/2}) peak. The result of N(1s) peak synthesis on the quaternarised Burning Star asphaltene is shown in Figure 1. The amount of pyridinium ion calculated from the iodine peak is in excellent agreement with that calculated by N(1s) peak synthesis alone, validating the N(1s) peak assignments. As a check of the XPS results, the basic nitrogen contents of some of the asphaltene fractions were determined by potentiometric titration. The amount of basic nitrogen determined directly agrees well with the XPS results (correlation coefficient 0.95), further confirming the validity of the XPS procedure. XPS, however, unlike the titration method, is not limited by the solubility of the samples.

ii) Infra-Red Spectroscopy

Since a simple two component model was found to fit the XPS data for all samples, the pyrrole to pyridine ratios obtained in this way can be viewed with some certainty. The volatile nature of some of the lower molecular mass coal derived fractions, however, makes them difficult to study by XPS. Because of this, the pyrrole contents, as determined by XPS, were used to calibrate the infra-red NH stretch (3480cm⁻¹). Figure 2 shows the plot of absorbance versus the XPS determined NH concentration for the range of coal derived asphaltene fractions studied. Several of the samples were recorded over a range of concentrations to establish the validity of the Beer-Lambert relationship for these materials. The linearity of these plots indicates that the solutions were sufficiently dilute to prevent significant intermolecular hydrogen bonding. Using the Beer-Lambert law the specific absorption coefficient per gram of NH was calculated to be $6.9 \pm 0.4 \text{ dm}^3\text{g}^{-1}\text{cm}^{-1}$. With this value it is possible to use infra-red spectroscopy as an independent method of calculating [NH]. Furthermore, comparison of the XPS and FT-IR data obtained from shale oil asphaltene suggests that the extinction coefficient may be generally applicable to high molecular mass fossil fuel samples.

2) Analysis of Sulphur Containing Functional Groups

i) Temperature Programmed Reduction of Sulphur Functional Groups

The Beringen coal and its SRC product were analysed by temperature programmed reduction (TPR). The TPR kinetogram of the coal showed two resolved peaks at 380°C and 420°C, corresponding to the reduction of organic sulphur functional groups and pyrite respectively. In contrast to this, the TPR kinetogram of the SRC product obtained from the same coal contained no pyrite peak and the peak due to the reduction of the organic components was shifted to lower temperatures, consistent with a change in sulphur functional group distributions. From model compound data, this peak shift suggests the formation of aromatic sulphide groups from thiophene structures.

ii) XPS of sulphur containing functional groups

Since XPS can analyse for all elements except hydrogen and helium, it offers a potential method for the determination of sulphur functional groups in fossil fuels. Frost et al⁷ and Perry and Grint⁸ demonstrated that there was a correlation between surface and bulk sulphur contents over a range of coals. XPS has also been applied to the study of sulphur in diesel particulates⁹, and, more recently, to determine the role of sulphur compounds in liquid fuel stability¹⁰.

Analysis of the S(2p) spectra of of the coal-derived samples discussed in section 1 above reveals that in most cases sulphur is present in one valence state, with binding energies centred at between 162.4eV and 164.7eV, depending on the individual sample, and corresponding to various organic sulphur (II) types (i.e. thiols, sulphides, disulphides or thiophenes). As shown in Figure 3a, however, in some samples, two peaks were observed, one centred at 164.5eV and the other at 169.3eV. These correspond respectively to organic sulphur (II) and oxidised sulphur (IV and VI) species. Comparison of the binding energy of the oxidised sulphur peak (169.3eV) with those for model compounds¹¹⁻¹³ reveals that this peak is probably due to sulphones (R-SO₂-R). Jones et al¹¹ showed that the performic acid/ methanol oxidation of thiophene structures yields sulphones in a two step process which goes via the sulphoxide. The sulphur peak at 169.3eV may, therefore, be tentatively assigned to the oxidation products of thiophenes (or sulphides) in the original asphaltene.

From consideration of the chemical shift data for sulphur containing model compounds, it is apparent that the chemical shift range for the possible fossil fuel sulphur types is not as great as was observed for nitrogen species. Furthermore, the larger number of possible functional groups would complicate the analysis. It is unlikely, therefore that a simple analysis by peak synthesis methods will be as effective as it was for nitrogen functional groups. As sulphur can exist in several different stable oxidation states, however, there is a potentially greater S(2p) chemical shift range accessible. Figure 3b shows the S(2p) spectrum of the SRC asphaltene 'A', after reaction with methyl iodide in which sulphur (II) is converted to sulphur (IV). As with the nitrogen compounds, an obvious peak shift to higher binding energies is evident. This shift is consistent with the formation of a sulphonium salt of the form RR'S⁺Me I⁻. Clearly, derivatisation reactions of this type can be readily followed by XPS. If XPS analysis is combined with a suitable fractionation scheme, or a series of selective derivatisation/oxidation reactions, it will provide a method from which valuable information about the distribution of sulphur types in coal and its derivatives may be obtained.

ACKNOWLEDGEMENTS

The authors thank the Science and Engineering Research Council for support of this work through grants and CASE studentships (S. Wallace and M. Baxby).

REFERENCES

- 1) L. Theodore and A.J. Buonicore (eds.), "Energy and the Environment: Interactions", Vol. I, Part A, CRC Press Inc.
- 2) J.R. Katzer and R. Sivasubramanian, Catal. Rev. - Sci. Eng., 20(2), 155, 1979.
- 3) K.D. Bartle, W.R. Ladner, T.G. Martin, C.E. Snape and D.F. Williams, Fuel 58, 413, 1979.
- 4) S. Wallace, M.J. Crook, K.D. Bartle and A.J. Pappin, Fuel 65, 138, 1987.
- 5) K.D. Bartle, D.L. Perry and S. Wallace, Fuel Processing Technol. 15, 351, 1987.
- 6) R.T. Moore, P. McCutchan and D.A. Young, Anal. Chem. 23, 1639, 1951.
- 7) D.C. Frost, W.R. Leeder and R.L. Tapping, Fuel 53, 206, 1974.
- 8) D.L. Perry and A. Grint, Fuel 62, 1024, 1983.
- 9) D. Scheutzle, L.M. Skews, G.E. Fisher, S.P. Levine and R.A. Gorse, Anal. Chem. 53, 837, 1981.
- 10) M.C. Loeffler and N.C. Li, Fuel 64, 1047, 1985.
- 11) R.B. Jones, C.B. McCourt and P. Swift, in 'Proc. Int. Conf. Coal Sci., Dusseldorf', Verlag Gluckauf, Essen, 1981, p.657.
- 12) D.C. Frost, B. Wallbank and W.R. Leeder, in C. Karr Jr. (Ed.) "Analytical Methods for Coal and Coal Products", 1978, Vol. I, Academic Press, London, p.394.
- 13) H. Harker and P.M.A. Sherwood, Phil. Mag. 27, 1241, 1973.

TABLE I
Distribution of Nitrogen Functional Groups

	SRC Asph. 'A'		SCR Asph. 'B'		Burning Star Coal Liquid Asph.				
	Asph. Bases	Asph. Bases	Asph. Bases	Asph. Bases	Raw Coal (dmmf)	Asph. Bases	Quat. Bases	Non-Basic N	
C	85.3	67.3	82.8	79.4	81.7	84.1	48.0	65.1	81.0
H	6.9	7.1	6.2	6.2	5.7	6.4	4.3	4.2	6.1
N	3.1	5.7	2.5	6.7	1.5	1.7	2.8	1.9	1.6
S	-	-	-	-	2.0	2.1	4.4	2.9	1.7
H/C	0.97	1.27	0.90	0.94	0.84	0.91	1.06	0.77	0.90
N/C	0.03	0.07	0.03	0.07	0.02	0.02	0.05	0.03	0.02
% Pyrrolic	62	30	49	35	58	58	35	40	65
% Pyridinic	40	62	50	63	31	34	62	60	33

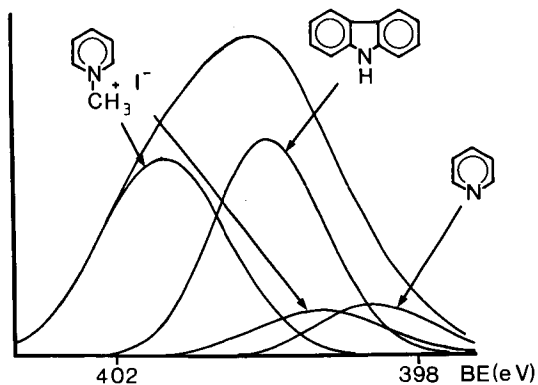


Figure 1. Synthesised N(1s) Spectrum of the Quaternarised Burning Star Asphaltene

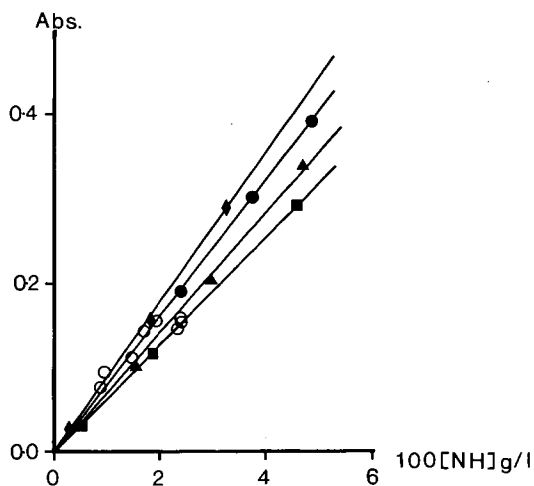


Figure 2. Plot of Absorbance Versus [NH] (Determined by XPS) for a Range of Coal Derived Asphaltene Fractions

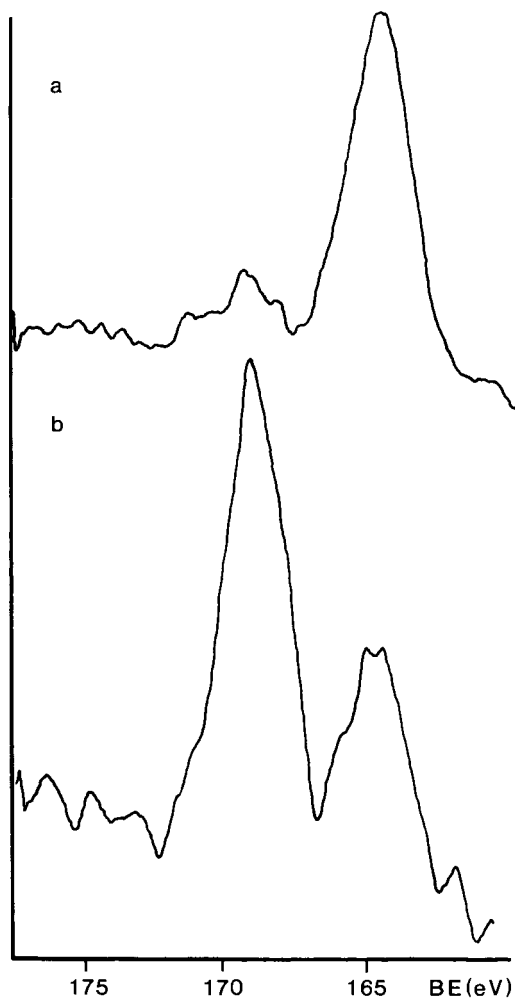


Figure 3. S(2p) Spectra of a) Asphaltenes and b) Quaternarised Asphaltenes

DIRECT DETERMINATION AND QUANTIFICATION OF SULFUR FORMS IN HEAVY PETROLEUM AND COALS. PART I: THE X-RAY PHOTOELECTRON SPECTROSCOPY (XPS) APPROACH

S. R. Kelemen, G. N. George, and M. L. Gorbaty

Exxon Research and Engineering Company, Route 22 East, Annandale, NJ 08801

Abstract

We have used the results from model compound studies to deconvolute the sulfur 2p signal from coal and heavy petroleum samples in the terms of the amounts of alkyl sulfides (163.3 eV) and thiophenic-like (164.1 eV) forms. The determination of organic sulfur forms in Illinois #6 coal was accomplished by carefully monitoring the contributions due to iron sulfides and sulfates and application of the deconvolution procedure used with heavy petroleum samples. Our results show that thiophenic-like sulfur comprises the majority of organic sulfur species in fresh Illinois #6 and Rasa coal. Analysis of Rasa coal following air oxidation show that organic sulfidic forms are much more reactive toward oxidation than thiophenic-like species.

I. Introduction

The routine direct quantification of organic sulfur forms in solids and nonvolatile liquids has not yet been accomplished; however, progress has been made using X-ray Adsorption Near Edge Structure (XANES) (1-2). The capability is important for understanding the chemistry of sulfur in coal and heavy hydrocarbons. It has been long recognized that XPS could potentially impact this characterization area for coal (3-8). The characterization of sulfur on coal surfaces by XPS is complex due to the presence of pyrite and other inorganic sulfur species. Other complications are that both organic and inorganic sulfur forms are susceptible to ambient oxidation and that the surface composition may not be representative of the bulk. Despite this awareness there has been very little detailed attention paid to contribution of inorganic sulfur forms. An XPS study (7) of many different coals observed only trace iron signals. The authors associated the 164.2 eV sulfur 2p peak with organic sulfur and attributed it to the sum of thiophenes, sulfides and mercaptans. This study (7) also demonstrated a reasonable correspondence between surface and bulk organic sulfur levels. Our approach to avoid the problems posed by the presence of inorganic sulfur was to establish XPS methods for quantitative determination of sulfur forms using model compounds and petroleum based materials. The same methods were then applied to a coal with a low pyrite and high organic sulfur content for characterization of sulfur forms. Finally a coal with equivalent amounts of pyrite and organic sulfur was analyzed for organic sulfur species after accounting for the contribution of inorganic sulfur forms to the XPS sulfur 2p signal.

II. Experimental

Illinois #6 coal was obtained from the Argonne premium coal sample program. The Rasa coal sample was obtained courtesy of Dr. Curt White at the Pittsburgh Energy Technology Center PETC. Polyphenylene sulfide was obtained from Scientific Polymer Products Inc. and all other model compounds were obtained from the Aldrich Chemical Company, Inc. XPS spectra were obtained with a Vacuum Generators ESCALAB instrument using non-monochromatic $MgK\alpha$ or $AlK\alpha$ radiation.

The petroleum samples were deposited from solution onto a metallic sample block. The coal and powdered model compound samples were mounted to the metallic sample block by means of double sided nonconducting tape. An energy correction was made due to sample charging for coal based on the C(1s) peak position observed at 284.8 ± 0.1 (eV) for the thin films ($<10\text{\AA}$ thickness) of heavy petroleum samples and THF extracts from Illinois #6 samples. These samples are believed to be in electrical contact with the metallic sample block. The spectra were obtained at 0.9 eV resolution. Data acquisition and processing were by means of the VGS 2000 software package. Oxidation experiments were done in air with ~60% relative humidity.

III. Results and Discussion

An idealized XPS sulfur 2p signal is made up of $2p_{3/2}$ and $2p_{1/2}$ components having 2:1 relative intensity and separated in energy by about 1.2eV. We have measured the XPS sulfur 2p signal from a variety of model compounds to obtain the instrumental response for a single component species as well as determine the binding energy representative of different sulfur environments. Figure 1 shows the spectra from several model compounds. We have found that the sulfur 2p signal can be represented by components having an equally mixed Gaussian-Lorentzian line-shape and a FWHM of 1.4 eV. Figure 1 curves A, B and E are examples which have this idealized line-shape. There is a very small peak at several eV higher binding energy than the main 2p signal in curves A and B. This emission is primarily a result of $\pi \rightarrow \pi^*$ shake-up processes (9). We can identify departures from what would be expected for a pure component material. There is a slight broadening of the sulfur 2p signal in Curve C for 2-methyl-L-cysteine; however, the sample is only of 97% purity. The broadening of the higher binding energy peak from the partially oxidized FeS_2 sample, curve D, reflects the presence of oxidized sulfur in environments with slightly different apparent binding energy.

The XPS sulfur 2p binding energy provides a sensitive measure of the electronic character of sulfur within a molecule. (10-12) The binding energies of oxidized organic sulfur forms are fairly well established (8-14) i.e. sulfoxides (~166 eV), sulfones (~168 eV) and sulfonic acid/sulfate (~169 eV). Figure 1 curve E is the sulfur 2p spectrum from dibenzothiophene sulfone which shows a binding energy 168.2 ± 0.1 eV. This agrees favorably with the values reported for sulfone in different polymeric materials (9). The details of the surface oxidation of FeS_2 are complex and will be discussed in greater detail later. The sulfur 2p spectrum of partially oxidized FeS_2 is shown in Figure 1 curve D. The lower binding energy peak occurs at 162.5 eV and is consistent with previously reported values for pyritic sulfur (15-19) which range from 162.3 eV to 163.0 eV. The higher binding energy peak occurs at 168.6 eV and is associated with sulfate. Sulfate was observed as a surface product following air oxidation of pyrite with binding energies of 168.5 eV (19) and 169.1 eV (16). These values are close to those anticipated for ferrous and ferric sulfate (12). Indeed we find the binding energy of ferrous sulfate at 168.9 eV. Brion (16) found 169.4 eV and 169.5 eV for ferric and ferrous sulfate respectively. Values as high as 171.0 eV and 172.2 eV have been published (4, 6) for ferric and ferrous sulfate respectively; however, no attempt was made to account for sample charging in these studies. The binding energy for polyphenylene sulfide in Curve B is 163.7 ± 0.1 eV which quantitatively agrees with a previous finding (9). The 164.1 eV binding energy for sulfur in a thiophenic-like environment (Tilorone Analogue) also agrees with that found for thiophene (12). We find a 163.3 eV binding energy for an alkyl sulfide containing

molecule S-methyl-L-cysteine.

We have measured the XPS sulfur 2p signal from several heavy petroleum samples. The XPS sulfur 2p signal for a single species, based on the instrumental response of pure model compounds, was used in a deconvolution procedure. It was possible in all cases to deconvolute the spectrum from petroleum asphaltene samples into two signals with binding energies of 164.1 eV and 163.3 eV (23). This observation was interpreted in light of available model compound results. The 163.3 eV component is representative of mostly sulfidic forms while the 164.1 eV corresponds to thiophenic-like environments.

We have analyzed the XPS sulfur 2p signal from fresh Rasa lignite coal. The spectrum is shown in Figure 2. It is an unusual coal, having very high levels of organic sulfur (11.68 wt%) and very little inorganic sulfur. The sulfur to carbon atom ratio as determined by XPS was in excellent agreement with that determined by elemental analysis. As we found with petroleum asphaltene, it was possible to deconvolute the main sulfur 2p peak into 164.1 and 163.3 eV components. The 164.1 eV peak makes up 70% of the signal and is assigned to organic sulfur species in thiophenic-like environments. Air oxidation for 5 days at 125°C changes the sulfur 2p spectrum as shown in Figure 3. The presence of oxidized sulfur forms is apparent at high binding energies and these forms make up about 24% of the total sulfur on the surface of Rasa coal. Upon oxidation, the amount of thiophenic-like components remains nearly constant, but the sulfidic components drop dramatically. The distribution of sulfur forms remains about the same following subsequent oxidation in air at 125°C up to 60 days. These results show that the thiophenic-like sulfur components in Rasa lignite are much less reactive toward oxidation relative to sulfidic forms.

Accounting for possible inorganic sulfur forms is essential for an accurate determination of organic sulfur surface species in pyrite containing coals. Figure 4 Curve A shows the iron 2p spectrum from Illinois #6 coal. The Illinois #6 sample was obtained from the Argonne premium sample program in a sealed ampule. The sample was prepared in an N₂ dry box, placed in a sample transfer device, evacuated and then inserted into the VG fast entry air lock for XPS sample analysis. The procedure nearly eliminated exposure to laboratory air. About half of the bulk sulfur in this coal is present as pyrite. The XPS iron spectrum contains a number of peaks that will be identified on the basis of 2p_{3/2} and 2p_{1/2} components from at least two distinct chemical forms. We can identify a sharp iron 2p_{3/2} peak at 708.5 eV and another very broad 2p_{3/2} peak at 713.5 eV. The energies were determined after correction for sample charging based on the C(1S) coal peak. Notice that the corresponding sulfur 2p spectrum, shown in Figure 5 Curve A, does not possess an easily discernible sulfate peak. The sulfur 2p signal appears over the energy loss envelope from the silicon 2s line. The maximum of this broad energy loss envelope occurs near 178 eV.

Careful studies on the surface oxidation of pyrite have shown that initial air oxidation products are an iron deficient sulfide, iron oxides and/or ferric sulfate (19). The binding energy of the metal-deficient sulfide is believed to be similar to unaltered pyrite (19), -707 eV (15-19). Iron oxides and ferric sulfate occur at -711 eV. We have measured a binding energy of 711.0 eV for ferrous sulfate. Sulfate was observed (19) by XPS as a later oxidation product of pyrite exposed to air. No evidence was found for the presence of elemental sulfur up to 14 day air exposure (19); however, elemental sulfur is an observed component in weathered coal samples (26).

The iron $2p_{3/2}$ binding energies from Illinois #6 coal cannot be chemically interpreted in a straight-forward way because the value falls outside of known limits. To conform to accepted values, the inorganic components would have to experience enhanced sample charging of about 1.0eV to 3.0eV relative to the main organic carbonaceous components. The possibility of enhanced sample charging for inorganic components in coal has been noted before (24,25). If we assume nonuniform sample charging, then the 708.2 eV peak is assigned to iron pyrite or the metal deficient sulfide shifted by ~ 1.2 eV and the broad peak at ~ 713.5 eV to iron oxides and/or sulfates shifted by ~ 2.5 eV. It would follow that the ~ 722 eV feature is due to the $2p_{1/2}$ peak from pyrite and the broad 727eV peak due to $2p_{1/2}$ from iron oxides and/or sulfates. These results show that the substantial portion of the observable iron from a fresh sample surface of Illinois #6 coal is non-pyritic in nature and in poor electrical contact with the organic matrix.

When the XPS sulfur 2p signal from iron pyrite is shifted by 1.2eV toward higher binding energy, it will directly overlap the region for unoxidized organic sulfur species. The total amount of iron present, as determined by the combined area of the $2p_{3/2}$ peaks from all iron species relative to the total amount of carbon, is only about a third of the amount determined by bulk analysis ($Fe/C = 0.0071$). Lower than expected iron XPS signals have been noted before (7). Two possible explanations are that the pyrite particles are encapsulated by organic material or that they have a particle size distribution significantly greater than the carbonaceous matter. The pyritic $2p_{3/2}$ peak is only 20% of the total $2p_{3/2}$ iron signal. We would, therefore, expect a pyritic XPS sulfur 2p signal that corresponds to a relative intensity of ($S/C=0.001$) or about 7% of the total sulfur 2p signal. The apparent binding energy of pyritic sulfur would be 163.7 eV due to enhanced sample charging. The pyritic XPS $2p_{3/2}$ signal decreases substantially upon exposure to air. Figure 4 curve B shows the decline in the iron $2p_{3/2}$ signal and Figure 5 curve B shows the appearance of a very small sulfate peak near 171.5 eV after a two day exposure to air at 22°C and $\sim 60\%$ relative humidity. Pyritic sulfur is initially present in very small quantities at surfaces of fresh Argonne premium Illinois #6 samples and the amount declines further upon exposure to air.

It was possible to deconvolute the XPS organic sulfur 2p signal from Illinois #6 coal using the same methods as used with Rasa coal and heavy petroleum samples after consideration of the pyritic sulfur contributions as just described and background subtraction of the silicon 2s signal. Figure 6 shows the results. The 164.1 eV peak contributes 64% and the 163.3 eV peak 29% to the total signal. These peaks are interpreted to arise from thiophenic-like and alkyl sulfide environments respectively. These results show that organic sulfur species dominate the XPS sulfur 2p spectrum of fresh Illinois #6 coal and that about 2/3 of the surface organic sulfur exists in thiophenic-like environments.

IV. Conclusions

It is possible to deconvolute the organic XPS sulfur 2p spectrum of coal and heavy petroleum samples into 163.3 eV and 164.1 eV components. These peaks have been interpreted in terms of alkyl sulfides and thiophenic-like sulfur species respectively. Thiophenic-like sulfur represents the majority organic species in Rasa and Illinois #6 coal. Air oxidation of Rasa coal results in the loss of organic sulfides and the production of oxidized species. Detailed analysis of the iron and sulfur XPS sulfur 2p signals shows that inorganic

sulfur species represent a very small fraction of the total sulfur present on surfaces of fresh Argonne Premium Illinois #6 coal.

References

1. George, G.N. and Gorbaty, M.L. J. Am. Chem. Soc. (1989), in press.
2. Huffman, G.P., Higgins, F.E., Mitra, E., Shah, N., Pugmire, R.J., Davis, B., Lytle, F.W., and Greeger, R.B. Energy and Fuels 3 (1989) 200.
3. Schultz, H.D. and Proctor, W.G. Applied, Spectroscopy 27 (1973) 347.
4. Frost, D.C., Leeder, W.R. and Tapping, R.L., Fuel 53 (1974) 206.
5. Frost, D.C., Leeder, W.R., Tapping, R.L. and Wallbank, B., Fuel 56 (1977) 277.
6. Samarendra, N., Dutta, N. and Frost, D.C., Fuel 62 (1983) 840.
7. Perry, D. L. and Grint, A. Fuel 62 (1983) 1029.
8. Jones, R.R., McCourt, C.B. and Swift, P. Proc. Int. Conf. Coal Sci. Dusseldorf (1981) 657.
9. Gardella, J.A., Jr., Ferguson, S.A., and Chin, R.L., Applied Spectroscopy 40 (1986) 224.
10. Siegbahn, K., Phil. Trans. R. Soc. London. A 268 (1970) 33.
11. Gassman, P.G., Callstrom, M.R., Martin, J.C. and Rongione, J.C., J. Am. Chem. Soc. 110 (1988) 8724.
12. Wagner, C.D., Rigg, W.M., Davis, L.E., Moulder, J.F. and Muhlenberg, G.E., Handbook of X-ray Photoelectron Spectroscopy (Perkin-Elmer Corporation, Eden Prairie, MN, 1979).
13. Clark, D.T., and Munro, H.S., Polymer Degradation and Stability 8 (1984) 213.
14. Thomas, H.R., Ph.D. Thesis, University of Durham, U.K. (1977).
15. Van der Heide, H., Hemmel, R., VanBruggen, C.F., and Haas, C. J. Solid State Chem. 33 (1980) 17.
16. Brion, D. Appl. Surf. Sci 5 (1980) 133.
17. Ennaoui, A., Frechter, S., Jaegermann, W. and Tributsch, H., J. Electrochem. Soc. 133 (1986) 97.
18. Jaegermann, W. and Tributsch, H., J. Appl. Electrochem. 13 (1983) 743.
19. Buckley, A.N., and Woods, R., App. Surf. Sci. 27 (1987) 437.
20. Clark, D.T. and Wilson, R., Fuel 62 (1983) 1034.

21. Clark, D.T., Wilson, R., and Quirke, J.M.E., Chem. Geol. 39 (1983) 215.
22. Clark, D.T., and Wilson, R., Org. Geochem. 6 (1984) 455.
23. Kelemen, S.R., George, G.N., Gorbaty, M.L., Fuel Process Technol. in press.
24. Kelemen, S.R., and Freund, H. ACS Fuel Div. preprints 33 (1988) 706.
25. Weitzsacker, C.L., Schmidt, J.J. and Gardella, J.A., Jr., ACS Fuel Div. preprints 34 (1989) 545.
26. Duran, J.E., Mahasay, S.R. and Stock, L.M., Fuel 65 (1986) 1167.

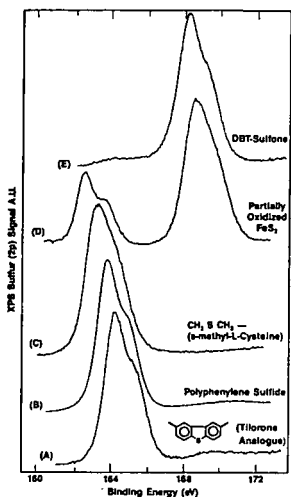


Figure 1
XPS sulfur 2p spectra
from model compounds.

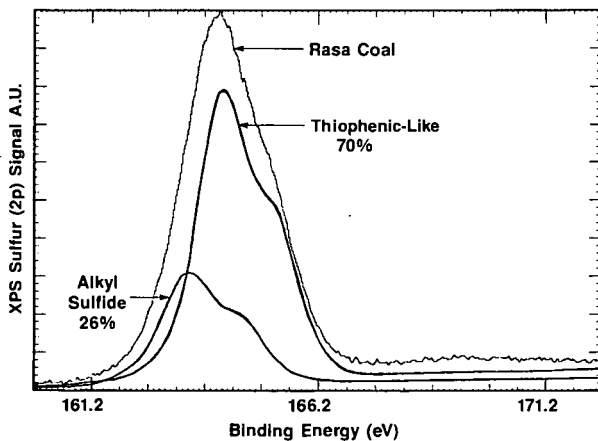


Figure 2 XPS sulfur 2p spectrum from fresh Rasa coal and deconvolution into 163.3eV and 164.1 eV components.

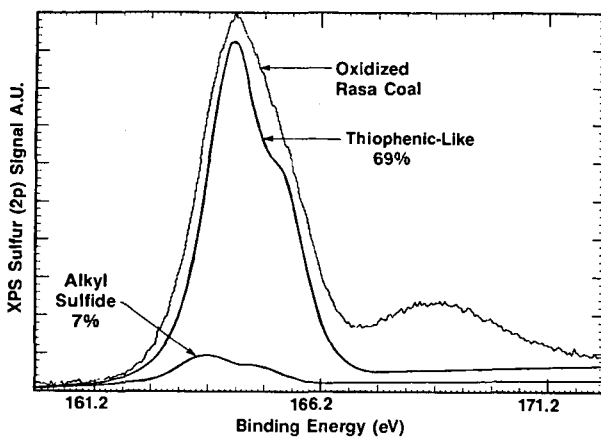


Figure 3 XPS sulfur 2p spectrum from Rasa coal oxidized for 5 days at 125°C and deconvolution into 163.3 eV and 164.1 eV components.

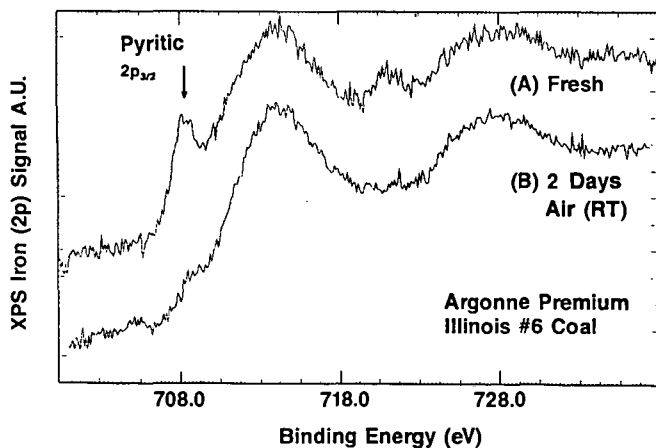


Figure 4 XPS iron 2p spectra from Argonne Premium Illinois #6 coal: a) Fresh; b) after air exposure at 22°C for 2 days

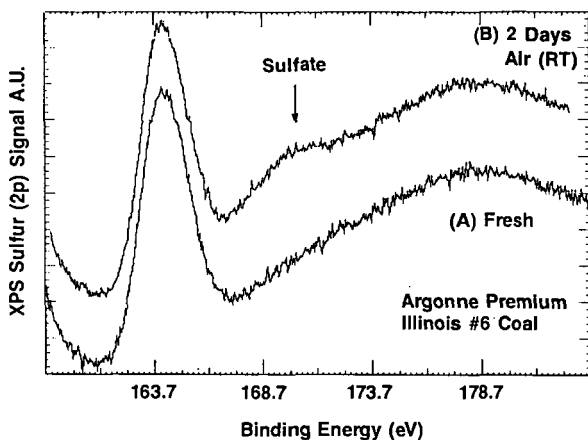


Figure 5 XPS sulfur 2p spectra from Argonne Premium Illinois #6 coal; a) Fresh; b) after air exposure at 22°C for 2 days.

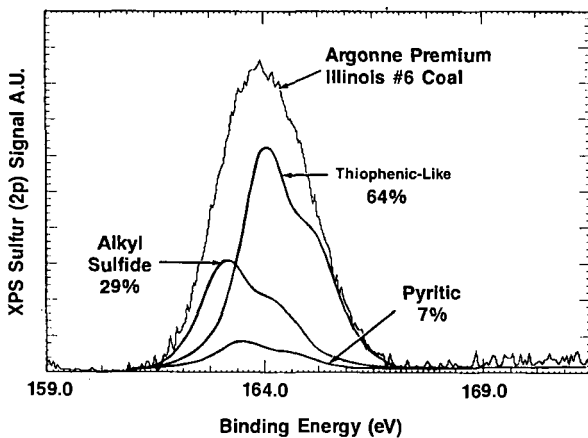


Figure 6 XPS sulfur 2p spectrum from fresh Illinois #6 coal and deconvolution into different components.

DIRECT DETERMINATION AND QUANTIFICATION OF SULFUR FORMS IN HEAVY
PETROLEUM AND COALS. PART II: THE SULFUR K EDGE X-RAY ABSORPTION
SPECTROSCOPY APPROACH

Martin L. Gorbaty, Graham N. George and Simon R. Kelemen
Exxon Research and Engineering Company
Annandale, NJ 08801

ABSTRACT

A Sulfur K Edge X-ray Absorption Spectroscopy method has been developed for the direct determination and quantification of the forms of organically bound sulfur in nonvolatile petroleum and coal samples. XANES spectra were taken of a number of model compounds, mixtures of model compounds, heavy petroleum and coal samples. A third derivative analysis of these spectra allowed approximate quantification of the sulfidic and thiophenic components of the model mixtures and of heavy petroleum and coal samples.

INTRODUCTION

Although many attempts have been made to determine the forms of organically bound sulfur in nonvolatile and solid hydrocarbonaceous materials, virtually all have involved in one way or another some chemical change to the structures, and leave open questions as to what is being measured (1). While less of an issue for petroleum based samples (2), chemical derivatizations of coal require good mass transport to be sure that the reaction is complete and all products are accounted for. Pyrolysis type experiments (3a) leave open the question as to whether sulfur forms are interconverting (3b). To remove these ambiguities, a direct measurement is required, which must be element specific, environment sensitive, and must be able to observe the entire sample. X-ray Absorption Spectroscopy (XAS) is one such method. In earlier work Hussain et al. (4), Spiro et al. (5), and later Huffman et al. (6,7) demonstrated the potential of sulfur X-ray absorption spectroscopy for the qualitative determination of sulfur forms in coals, however they made no attempt at quantification. This report investigates the applications of X-ray absorption near edge spectroscopy (XANES) for the purpose of speciating and quantifying the forms of organic sulfur in solids and nonvolatile liquids.

EXPERIMENTAL SECTION

The details of the XANES experimental setup and data analyses have been described previously (3b,8). All model compounds used in this study were obtained from Aldrich Chemical Company and were used without further purification. The asphaltene samples were prepared from their respective petroleum residues by precipitation from n-heptane following the procedure of Corbett (9). A sample of Rasa lignite was generously provided by Dr. Curt White. The sample of Illinois #6 coal was obtained from the Argonne Premium Coal Sample Bank.

RESULTS AND DISCUSSION

XANES of Model Compounds

Table 1 lists the first inflection points of the sulfur K edge spectra for a series of model compounds whose structures are believed to be representative of the types of organically bound sulfur found in heavy petroleum and coals. Although the absolute value for the energy calibration contains some uncertainty, the relative accuracy of the energy scale proved to be reproducible to within less than 0.1 eV. The total span in energy is quite large, being some 12.4 eV between thiohemianthraquinone and potassium sulfate. As might be anticipated (10,11), the first inflections of compounds with more oxidized sulfur are notably higher in energy than for those with reduced sulfur. The sulfur XANES spectra of compounds with similar sulfur electronic environments were found to be similar. For example, dibenzothiophene and benzothiophene were found to give similar sulfur XANES spectra, whereas dibenzothiophene and thianthrene, whose sulfur atoms are in significantly different environments, exhibit dissimilar sulfur XANES.

Examination of Table 1 reveals that the edge of dibenzothiophene is displaced from that of benzyl sulfide, the first inflection energy being some 0.6 eV higher for the former compound. The XANES spectra of the compounds listed in Table 1 (3b,8) can readily be used as a fingerprint for the electronic nature of organically bound sulfur, and for distinguishing between the forms of sulfur in the pure compounds. From previous XANES data on dibenzothiophene and benzyl sulfide and physical mixtures of the two, it proved possible to identify each compound in the presence of the other (3b,8). Additionally by simply measuring the heights of the third derivative features at 2469.8 eV and 2470.8 eV relative to the base line in the model compound mixtures, a calibration was established which allowed an approximate estimate of the amounts of each component in hydrocarbon samples to be obtained.

XANES of Petroleum Residua

On the left side of Figure 1 the sulfur K edge spectra for three different petroleum residua and the asphaltene samples prepared from them are shown. While the absorption spectra all appear to be similar, differences are revealed by examining the third derivatives of the spectra, which are shown on the right side of the figure. All the residua samples appear to contain sulfur bound in sulfidic and thiophenic forms, the amount of sulfidic sulfur increasing from sample 1 to sample 3. The asphaltene samples prepared from residua 2 and 3 also appear to contain both forms. Assuming that the composition of the sulfur forms in these samples is approximated by the simple two component mixture of dibenzothiophene and dibenzylsulfide models, an estimate of the relative molar quantities of sulfidic and thiophenic forms can be obtained as described above. These approximate values are listed in Table 2. In samples 1 and 3, it is clear that the predominant form of sulfur in the asphaltene fractions is thiophenic and the predominant form in the whole residuum is sulfidic. For sample 2, there appears to be no such discrimination.

In the latter case, the totals do not add to 100%. While thickness effects may play a role, a more probable explanation for this observation is that a range of slightly different sulfur types, of both sulfidic and thiophenic forms exist in this material, which causes a broadening of the features of the XANES spectrum and making quantification based on mixtures of two model compounds less

accurate. In agreement with this the structure of the third derivative spectra of both the resid sample 2 and the asphaltene derived from it do appear to be broadened relative to that of the spectra of sample 3 in Figure 1. Since the broadening takes place in the "sulfidic" region, both data sets were normalized to 100%, giving a rough approximation of the amounts of sulfidic and thiophenic sulfur, which are shown in parentheses in the table.

XANES of Coal

In Figure 2 are shown the XANES spectra and their third derivatives of the Rasa lignite and Illinois #6 coal samples, and Table 2 the approximate quantification of sulfur types. The former coal was chosen for this study because it has an unusually high amount of organically bound sulfur, and an unusually low level of pyritic sulfur (12). The latter was chosen because its relatively high pyritic sulfur content provides a means of defining to what extent pyritic sulfur interferes with data interpretation.

For Rasa lignite, this XANES analysis indicates that about 30% of the sulfur is sulfidic and 70% is thiophenic. These numbers are in agreement with those found by XPS (14). Partial confirmation of these values also comes from the work of Kavcic (13), who showed that about 75% of the sulfur in this lignite was not reactive toward methyl iodide; this lack of reactivity was attributed to the sulfur being bound in ring structures. Even recognizing the potential or inherent errors of the methyl iodide method such as degree of reaction, possible side reaction, etc., the extent of agreement of the direct and indirect techniques is good.

The XANES spectrum for the Argonne Premium Illinois #6 coal and its third derivative in Figure 2 clearly show that pyritic sulfur is a significant component. As a first step to extract data on the organic sulfur content, the XANES spectrum of iron pyrite (determined separately and not shown in the figure) was mathematically subtracted from the XANES spectrum of the coal. The resulting spectrum and its third derivative are shown in Figure 2 below those of the whole coal, and from this third derivative approximate quantifications of 60% sulfidic and 40% thiophenic sulfur forms were determined (Table 2). It is interesting to note that these are in reverse order from what was found by XPS analysis on this same coal (14) and on another Illinois #6 sample by pyrolysis techniques (3a). The XANES approximations for this coal should be considered as tentative and subject to change due to possible errors in the subtraction method used. For example, if the pyrite actually present in the coal has different spectral characteristics than the pyrite sample examined by XANES, the sulfidic numbers could be higher than actual. Work is in progress to better define the interference effects of pyritic sulfur. It is interesting to note that if these data are shown to be valid, comparison with data obtained by pyrolysis would imply that sulfidic sulfur can interconvert to some extent to thiophenic sulfur on heating.

CONCLUSIONS

This work has demonstrated that organically bound sulfur forms can be distinguished and in some manner quantified directly in model compound mixtures, and in petroleum and coal. The use of the third derivative XANES spectra was the critical factor in allowing this analysis. The tentative quantitative

identifications of sulfur forms appear to be consistent with the chemical behavior of the petroleum and coal samples, although large amounts of pyritic sulfur may interfere with the accuracy. Further work is in progress to resolve the pyritic sulfur question and to extend these techniques to other nonvolatile and solid hydrocarbon materials.

ACKNOWLEDGEMENTS

X-ray absorption spectra were recorded at the Stanford Synchrotron Radiation Laboratory, which is funded by the Department of Energy, under contract DE-AC03-82ER-13000, Office of Basic Energy Sciences, Division of Chemical Sciences and the National Institutes of Health, Biotechnology Resource Program, Division of Research Resources. The writers wish to thank Dr. Curt White (PETC) for providing a sample of Rasa lignite, and Dr. K. Vorres (Argonne) for the sample of Illinois #6 coal.

REFERENCES CITED

1. Van Krevelen, D.W. *Coal*, Elsevier, Amsterdam, 1961, 171.
2. Rose, K.D. and Francisco, M.A., *J. Amer. Chem. Soc.*, 1988, 110, 637.
3. (a) See for example Calkins, W. H., *Energy Fuels*, 1987, 1, 59.
(b) George, G. N., Gorbaty, M. L., and Kelemen, S. R., in "Geochemistry of Sulfur in Fossil Fuels", ACS Symposium Series, in press.
4. Hussain, Z., Umbach, E., Shirley, D.A., Stohr, J. and Feldhaus, *J. Nucl. Instrum. Methods*, 1982, 195, 115.
5. Spiro, C.L., Wong, J. Lytle, F.W., Greegor, R.B., Maylotte, D.H. and Lamson, S.H., *Science*, 1984, 226, 48.
6. Huffman, G.P., Huggins, F.E., Shah, N., Bhattacharyya, D., Pugmire, R.J., Davis, B., Lytle, F.W. and Greegor, R.B., in "Processing and Utilization of High Sulfur Coals II", Chugh, Y. P. and Caudle, R. D., eds. Elsevier, Amsterdam, 1987, 3.
7. Huffman, G.P., Huggins, F.E., Shah, N., Bhattacharyya, D., Pugmire, R.J., Davis, B., Lytle, F.W. and Greegor, R.B., *ACS Division of Fuel Chemistry Preprints*, 1988, 33, 200.; Huffman, G.P., Huggins, F.E., Mitra, S., Shah, N., Pugmire, R.J., Davis, B., Lytle, F.W. and Greegor, R.B., *Energy Fuels*, 1989, 3, 200.
8. George, G. N. and Gorbaty, M. L., *J. Amer. Chem. Soc.*, 1989, 111, 3182.
9. Corbett, L.W., *Anal. Chem.*, 1969, 41, 576.
10. Frank, P., Hedman, B., Carlson, R.M.K., Tyson, T., Roe, A.L., Hodgson, K.O., *Biochemistry*, 1987, 26, 4975.
11. Bianconi, A., in "X-ray Absorption", D.C. Koningsberger, and R. Prins, eds., John Wiley & Sons, New York. 1988, 573.

12. Given, P. H., Prog. Energy Combust. Sci., 1984, 10, 149.; Ignasiak, B.S., Fryer, J. F. and Jadernik, P., FUEL, 1978, 57, 578, and references cited therein.
13. Kavcic, R., Bull. Sci. Conseil Acad. RPF, Yugoslav, 1954, 2, 12.
14. Kelemen, S. R., George, G. N., and Gorbaty, M. L., ACS Div. Fuel Chem. Preprints, 1989, 34, in press.

TABLE 1
Sulphur K edge First Inflection Energies (b)

Compound	First Inflection (a) (eV)
K2SO4	2478.5
anthraquinone 6-sulfonate(Na)	2477.6
tetramethylenesulfone	2475.6
diphenylsulfone	2474.8
dibenzothiophenesulfone	2474.7
dimethyl sulfoxide	2472.8
tetramethylenesulfoxide	2472.4
2-methylthiophene	2470.6
benzothiophene	2470.4
dibenzothiophene	2470.4
methionine	2470.3
thianthrene	2470.2
dioctylsulphide	2470.1
cystine	2470.1
tetramethylthiophene	2470.0
benzylphenylsulphide	2469.9
dibenzylsulphide	2469.8
2-naphthalenethiol	2469.8
cysteine	2469.2
diphenyldisulphide	2469.2
dibenzyliddisulphide	2469.1
sulfur	2469.1
iron pyrite	2468.4
thiohemianthraquinone	2466.1

- a. First inflection points were obtained from the position of the lowest energy maximum of the first derivative, and are considered accurate to better than 0.1eV.
- b. Modified from Reference 8.

TABLE 2
Approximate Quantification of Organically Bound Sulfur Forms in Heavy Hydrocarbons

<u>Sample</u>	<u>% Sulfidic (± 10)</u>	<u>%Thiophenic (± 10)</u>
<u>Petroleum</u>		
Residuum 1	29	71
Asphaltene 1	0	100
Residuum 2	42(58)	30(42)
Asphaltene 2	43(54)	37(46)
Residuum 3	65	35
Asphaltene 3	50	50
<u>Coal</u>		
Rasa lignite	30	70
Illinois #6 (APSB)	60	40

Figure 1

S K-edge XANES and 3rd. Derivatives of Petroleum

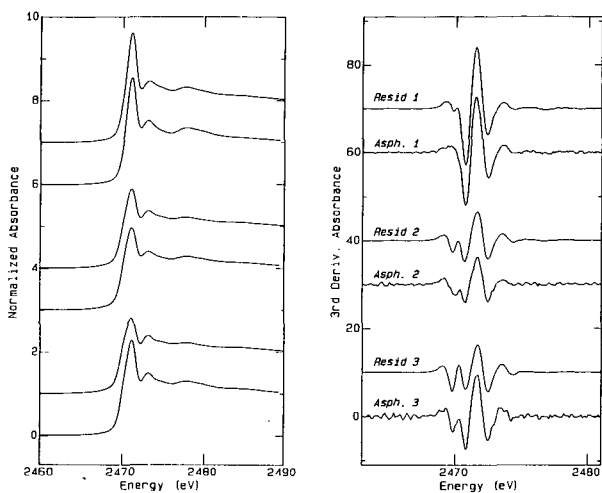
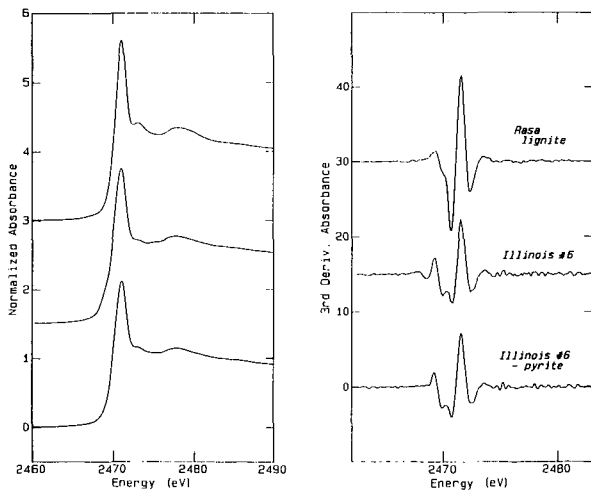


Figure 2

S K-edge XANES of Coals



IDENTIFICATION OF THE HETEROATOM CONTAINING COMPOUNDS IN THE
BENZENE/METHANOL EXTRACTS OF THE ARGONNE PREMIUM COAL SAMPLES

Paul H. Neill, Yun ju Xia† and Randall E. Winans

Chemistry Division, Argonne National Laboratory
9700 S. Cass Avenue, Argonne, Illinois 60439

The Argonne Premium Coal Samples (APCS) provide a unique opportunity to study a set of pristine samples specifically selected to represent the vast diversity of chemical structures exhibited by U.S. coals. The purpose of this paper is to utilize high resolution mass spectrometry (HRMS) to characterize the heteroatom containing species that can be extracted from the APCS. Of special interest is the change in structure and relative concentrations that these compounds undergo with rank. The resulting information is important in providing basic chemical structural information concerning these coals which are being used by a significant portion of the coal community, and understanding the transformations that the heteroatom containing species undergo during the coalification process.

EXPERIMENTAL

The coals used in this study and their elemental analyses are presented in Table I and the preparation of the coals has been described in detail by Vorres and Janikowski¹. The sample handling and extraction procedures along with an overview of our overall analysis scheme have been presented previously².

Table I. Elemental analysis of the APCS coal samples used in this study.

APCS Number	Coal	Carbon	Hydrogen	Nitrogen	Sulfur _{org}	Oxygen _{diff}	Extract Yield
8	Beulah-Zap	72.9	4.83	1.15	0.70	20.34	2.0
2	Wyodak Anderson	75.0	5.35	1.12	0.47	18.02	5.3
3	Illinois #6	77.7	5.00	1.37	2.38	13.51	8.2
6	Blind Canyon	80.7	5.76	1.57	0.37	11.58	7.5
7	Lewiston-Stockton	82.6	5.25	1.56	0.65	9.83	3.1
4	Pittsburgh	83.2	5.32	1.64	0.89	8.83	3.7
1	Upper Freeport	85.5	4.70	1.15	0.74	7.51	0.5
5	Pocahontas #3	91.0	4.44	1.33	0.50	2.47	1.9

However, a brief overview the experimental procedure is appropriate here. One hundred grams of the -100 mesh dried coal was extracted for 48 hours in 250 ml of boiling benzene/methanol azeotrope (40/60 w/w percent). The extract was removed by vacuum filtration, the residue was washed with 50 ml. of the azeotrope, and dried to constant weight at 100°C under vacuum. The two low rank coals (Wyodak Anderson and Beulah Zap) were extracted without drying in order to avoid irreversible physical or chemical changes that are known to occur during drying. The azeotrope was stripped from the extract at 70°C under vacuum in a rotary evaporator and the extract brought to constant weight. The two higher rank coals (Upper Freeport and Pocahontas #3) did not yield enough extract for subsequent separation.

†Present address: Department of Chemistry, Tsinghua University, Beijing, People's Republic of China.

The extract from the six lower rank coals was then separated into nine fractions using the desorption column chromatographic technique (DSEC) developed by Farcasiu^{3,4}. The eluants in order of use include: (1) hexane, (2) hexane/15% benzene, (3) chloroform, (4) chloroform/10% diethyl ether, (5) diethyl ether/3% ethanol, (6) methanol, (7) chloroform/3% ethanol, (8) tetrahydrofuran, (9) pyridine/3% ethanol. In our application of this technique the extract was dissolved in 7 ml. of the azeotrope and coated on 6.65 grams of dried silica gel by rotary evaporation of the solvent. The coated silica gel was placed on the top of the column containing 26.8 grams of Aldrich Grade 12 silica gel. This silica gel had been dried for 8 hours at 120°C and then rehydrated to 4 percent water. Blank elutions were performed in order to correct the weight of each fraction for dissolved silica gel.

For the high resolution mass spectra approximately 20 mg. of the extract from fractions 3-6 was dissolved in benzene/methanol azeotrope. 0.1 mg of the Diels-Alder adduct of D₁₀-anthracene and maleic anhydride was added as an internal standard and the resulting solution concentrated to 0.3 ml. The synthesis and applicability of this adduct as an internal standard in HRMS has been discussed previously⁵. The solution was placed on the tip of a glass probe and the solvent was allowed to evaporate. The probe containing the sample was inserted into the all glass inlet system held at room temperature and evacuated. The temperature of the inlet system was rapidly raised to 350°C and the volatilized sample was allowed to leak into the source of the Kratos MS 50 high resolution mass spectrometer. Approximately 10 scans were obtained for each sample at an electron ionizing energy of 70 eV, and a scan rate of 100 seconds/decade providing a dynamic resolution of 40,000. The resulting data was transferred to a Micro Vax II for final analysis. This analysis utilized a set of programs developed in house for averaging the scans in the run and assignment of elemental formulae to the averaged masses and sorting by heteroatom content and hydrogen deficiency (HD = rings + double bonds)⁶.

RESULTS AND DISCUSSION

The distribution of the extract in each of the DSEC fractions, for each of the coals for which enough extract was available, is shown in Figure 1. Although, no strict correlations are observed, several general conclusions can be drawn. The percentage of the total extract eluting in the hexane (1) and chloroform/10% diethyl ether (4) - Tetrahydrofuran (8) fractions tends to decrease with rank while the hexane/15% benzene (2) and chloroform (3) fractions increase. This is not particularly surprising since we know from elemental analysis that the amount of oxygen decreases with rank⁷ while the nitrogen content remains steady or increases only slightly⁸. Yarzab, Given and coworkers⁹ have shown that the phenolic content decreases with rank. However, a linear correlation is only observed with carbon content within a single coal province. The amount of extract eluting in the hexane (1) fraction shows the tendency to decrease with rank if the Blind Canyon coal is not considered. This coal is unusual in the fact that it exhibits an abnormally high liptinite content. Gas chromatography/mass spectrometry (GC/MS) of this fraction indicates that it is composed almost exclusively of alkanes and cycloalkanes. GC/MS and HRMS of the hexane/15% benzene (2) fraction indicated that only trace amounts of heteroatomic species are present. Thus, the remaining discussion in this paper will be limited to the chloroform (3) through methanol (6) fractions.

The degree of condensation increases with rank for each of the heteroatomic classes of compounds. Figure 2 illustrates this trend using single oxygen containing ions from the chloroform (3) fraction. The two low rank coals (Beulah Zap (#8) and Wyodak Anderson (#2)) are dominated by species with HD values less than 10. An HD of 10 corresponds to an anthracene or phenanthrene type structure if all of the rings are aromatized. A more likely assignment would be a smaller condensed structure with additional aliphatic or partially unsaturated rings. While the higher rank coals exhibit much larger contributions from ions with HD values in the range of 10-19. For the two highest rank coals for which we have data (Pittsburgh (#4) and Lewiston-Stockton (#7)), a maximum in the distribution is observed at HD=12. This corresponds to the empirical formula C₂₀H₁₈O for the base structure of the homologous series. This trend was also recognized by Given and coworkers who used catalytic dehydrogenation by Pd/CaCO₃ in boiling phenanthridine.¹⁰

Oxygen Compounds. Compounds containing one, two and three oxygens are present in the extracts from all of the coals. The distribution of these classes among the fractions are presented in Table II. Single oxygen containing species are found primarily in the chloroform (3) and chloroform/10% diethyl ether (4) fraction, two oxygen containing species in the chloroform/10% diethyl ether (4) and diethyl ether/3% ethanol (5) fractions, and three oxygen containing species in the methanol (6) fraction. Single oxygen carbonyl compounds of the type

investigated by Given and Peover¹¹ may also be present in this fraction. However, their unequivocal identification by HRMS is not possible.

The single oxygen compounds in the chloroform (3) fraction appear to be primarily phenolic in nature with maxima at HD 4, 7, and 10. While those in the chloroform/ether fraction produce a higher concentration of ions at HD= 3, 6, 9 which can be assigned to structures containing five membered rings or those containing several aliphatic or partially saturated six member rings. Since compounds of these two types are isomers it is not possible to distinguish between them by HRMS. An example of the HD distribution for these compounds was presented in Figure 2 above.

The two oxygen containing compounds which are found in every fraction are predominantly aliphatic carboxyl based (HD=1) for the low rank coal and dihydroxy or furan based for the coals of higher rank. The carboxyl containing compounds were found in each of the fractions for the lower rank coals but primarily in the methanol fraction (6) for the higher rank coals. The fragmentation pattern of the carboxyl compounds eluting in the less polar fractions indicate that they are most likely esters. These esters which were also observed by Bockrath et al.¹² could be either indigenous to the coal as suggested by Niwa et al.¹³ or formed during the extraction in benzene/methanol. This contradicts the work of Miller et al.¹⁴ who claimed that acids were present only lignites, low rank subbituminous and a few Rocky Mountain H_vC bituminous coals. In the low rank coals carboxylic acids are observed with carbon numbers up to 33 while in the higher rank coals the series ends at 6 carbons.

The three oxygen containing compounds appear primarily at HD= 4, 7, 10 which corresponds to fully aromatized compounds with three OH groups. However, the base compound is not found in the series from any of the coals. This leads to the conclusion that instead of being purely phenolic in nature the three oxygen compounds eluting in this fraction are at least partially alkoxy in nature. This is not surprising since purely phenolic three oxygen containing compounds would be very difficult to elute. Somewhat surprising is the amount of aliphatic, and partially unsaturated (HD<4) three oxygen compounds that are found in the methanol fraction. These compounds make up from 17 to 40 percent of all of the three oxygen compounds eluting in this fraction. The difficulty in rationalizing the presence of possible structures for these compounds in coal leads to the possibility that they are either contamination or mis-assignments.

Nitrogen Compounds. Single and double nitrogen containing species eluted primarily in the methanol (6) fraction, but trace amounts of one single nitrogen containing compounds were also observed in the chloroform (3) fraction. In the chloroform (3) fraction three series of alkylated condensed anisoles are present at HD= 6, 9, and 12 for the higher rank coals. Probable structures for these compounds include either the N, or highly hindered C, alkylated forms. Although a definitive conclusion can not be drawn, the discreteness of elution with

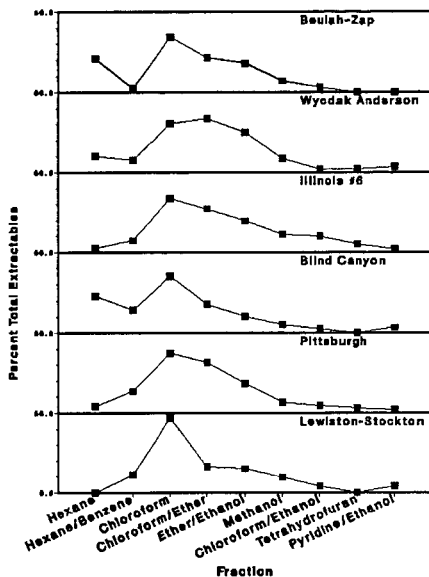


Figure 1. Distribution of the total extract in each of the DSEC fractions.

two interleaving fractions before the next appearance of compounds exhibiting the same elemental formula, leads to the conclusion that these are the N alkylated forms, as has been proposed previously¹⁵.

The ratio of HD=9/10 and 12/13 is plotted versus carbon content in Figure 4. Except for Illinois #6 coal the ratio decreases with rank. The interpretation of this figure is somewhat complicated by the fact that it is impossible to distinguish if the nitrogen is in the 5 membered ring or not. The plot does show that the relative degree of aromaticity increases with rank. Species containing two nitrogen compounds are present in the extract from all of the coals except Beulah Zap. The most prominent series of these compounds is found at HD=9. A series based on a second compound would have as its base the formula $C_{11}H_8N_2$, which was not observed. This corresponds to the formula $C_{12}H_{10}N_2$ for the base compound.

Sulfur Compounds. All of the extracts contained minor amounts of thiophenic compounds (HD= 6, 9, 12) which eluted in the ether/3% ethanol (5) fraction. Although sulfur is notoriously difficult to identify in HRMS, the small deviations from the expected mass, the generation of rational structures for annulated thiophenes versus irrational structures for alternative classes of compounds, and the observance of the expected HD distribution lead to the conclusion that the assignments are valid. The assignment of sulfur containing structures to possible matches at HD values other than those corresponding to thiophenes would be considerably more tenuous, due to the failure of at least two of the criteria mentioned above.

Mixed Heteroatomic. The mixed heteroatom containing compounds are found primarily in the diethyl ether (5) and methanol (6) fractions. The most prominent species from all of the coals are the hydroxylated pyridines, indoles and their higher order annulates. These compounds follow the same trend (see Figure 5) as that observed for the unhydroxylated indoles and pyridines, showing a decrease in the ratio of the 5 membered ring to that of the 6 membered ring with rank. A significant number of sulfur-nitrogen compounds may also be present in the methanol (6) fraction of the higher rank coals. These compounds are observed primarily at HD = 3, 4, 6, 7, 9, 10, 12, 13. However, as mentioned in the previous paragraph, compounds containing sulfur are notoriously difficult to assign structure due to their small mass defect. Hydroxylated thiophenes were not observed in any of the fractions.

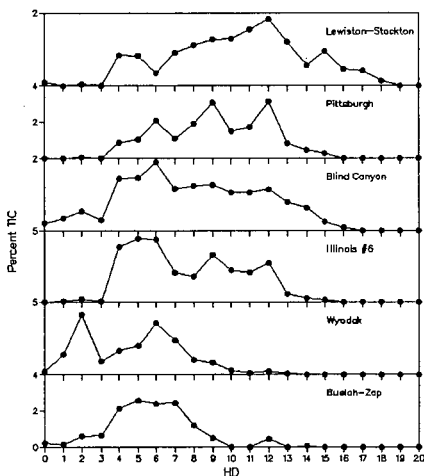


Figure 2. Variation in HD for single oxygen containing compounds in the chloroform (3) fraction.

Table II. Variation of one two and three compounds in DSEC fractions 3-6.

Coal	Chloroform (3)			Chloroform/10% Diethylethe (4)		
	One O	Two O	Three O	One O	Two O	Three O
Beulah Zap	13.2	2.7	0.0	15.3	1.0	0.1
Wyodak-Anderson	18.8	14.4	0.2	20.3	21.5	2.1
Illinois #6	28.3	2.4	1.5	33.9	6.4	1.4
Blind Canyon	14.8	2.2	0.3	12.2	12.4	1.9
Pittsburgh	18.1	0.3	4.0	50.1	5.0	2.7
Lewiston-Stockton	13.9	1.1	4.0	30.2	12.2	2.1

Coal	Diethyl Ether/3% Ethanol (5)			Methanol (6)		
	One O	Two O	Three O	One O	Two O	Three O
Beulah Zap	22.1	14.0	4.0	13.7	12.6	2.8
Wyodak-Anderson	19.0	21.9	5.5	12.3	11.7	4.8
Illinois #6	12.3	4.9	1.2	3.6	1.0	12.7
Blind Canyon	11.5	11.3	7.6	2.9	2.1	11.3
Pittsburgh	19.2	13.7	5.7	7.3	4.3	9.8
Lewiston-Stockton	11.3	8.3	4.8	5.6	1.6	9.4

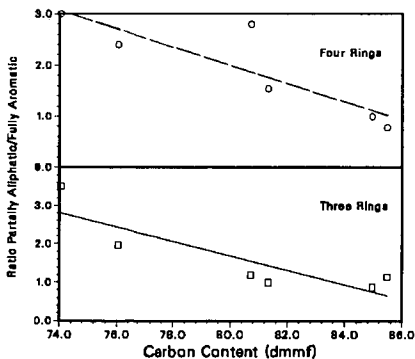


Figure 3. Ratio of HD 9/10 and 12/13 for the single nitrogen containing species in the methanol (6) fraction.

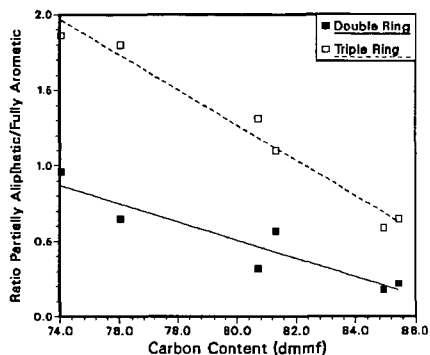


Figure 4. Ratio of HD 9/10 and 12/13 for the oxygen-nitrogen containing compounds in the methanol (6) fraction.

ACKNOWLEDGMENTS

The coal samples were provided by the Argonne Premium Coal Sample Program.

This work was performed under the auspices of the Office of Basic Energy Sciences, Division of Chemical Sciences, U.S. Department of Energy, under contract number W-31-109-ENG-38.

REFERENCES

1. K. Vorres and S. Janikowski, *ACS Fuel Division Preprints*, 32(1), 492, (1987).
2. Y.J. Xia, P.H. Neill, and R.E. Winans, *ACS Fuel Division Preprints*, 32(4), 1987, 340-346.
3. M. Farcasiu, *Fuel*, 56, 9, (1977).
4. D.D. Whitehurst, T.O. Mitchell, and M. Farcasiu "Coal Liquefaction: The Chemistry and Technology of Thermal Processes", Academic Press, New York, 1980, Chapter 3.
5. R.E. Winans, R.L. McBeth, and P.H. Neill, *ACS Fuel Division Preprints*, 33(3), 85, (1988).
6. R.E. Winans, R.G. Scott, and P.H. Neill, *Fuel Proc. Tech.*, 12, 77 (1986).
7. A. Volborth, G.E. Miller, C.K. Garner, and P.A. Terabele, *Fuel*, 57, 49, (1978).
8. J.P. Boudou, A. Mariotti, and J.L. Oudin, *Fuel*, 63, 1508, (1984).

9. Yarzab, R.F., Given, P.H., Davis, A. and Spackman, W., Fuel 59, 81-92 (1980).
10. Given, P.H., Duffy, L.J. and Binder, C.R., ACS Fuel Division Preprints, 7(2), 145, (1963).
11. Given, P.H. and Peover, M. E. Inst. of Fuel, London A-33-A-37 (1958) and J. Chem. Soc. 394-400, (1960).
12. B.C. Bockrath, K.T. Schroeder, and F.W. Steffgen, Anal. Chem., 51, 1168, (1979).
13. Y. Niwa, M. Yumura, K. Ishikawa, Y. Kuriki, and M. Kawamura, Fuel, 67, 98, (1988).
14. Miller, R.N., Yarzab, R.F. and Given, P.H. Fuel, 58, 4-10, (1979).
15. BETC US DOE, Quarterly Technical Report QPR-80/3, February 1981.

ANALYSIS AND COMPARISON OF TWO VICTORIAN BROWN COAL RESINITE SAMPLES¹

Ken B. Anderson*, R.E. Botto, G.R. Dyrkacz, R. Hayatsu, and R.E. Winans

Chemistry Division, Argonne National Laboratory,
9700 South Cass Avenue, Argonne, IL 60439

*Also, Department of Organic Chemistry, University of Melbourne,
Parkville, Victoria, Australia 3052

INTRODUCTION

Amongst the organic constituents of coal, the maceral resinite is probably the least complex structurally, due to the relatively simple composition of the original resins. Hence, with careful analysis, it may be possible to construct meaningful and accurate structural descriptions of this maceral. This is especially true of resinites found in low rank coals, where macroscopic resinite accumulations are relatively common, and in which the effects of catagenetic processes are minimal or absent.

For the purposes of this study, two physically diverse resinite samples were obtained from Victorian Brown Coal (VBC) by hand picking from open cut mine faces. The first sample, which is referred to as "resinite" throughout this text is a hard, brittle, glassy material, yellow/brown in colour. The second is a soft, brittle, bone white material, which was found in association with a large gymnosperm log, of undetermined paleobotanical affinity, as sheets between "wood" and "bark". This material is sometimes referred to as "bombicite" by geologists, and is referred to by this name in this text in the interests of clarity. Petrographically, both samples are classified as resinite.

EXPERIMENTAL

Pyrolysis-high resolution mass spectra were recorded on a Kratos MS-50 mass spectrometer, operating at a dynamic resolution of 10 000. Ramped pyrolyses (150-800°C, 50°C/min) were used for pyrolysis of these resins in order to minimize thermal reactions in volatile products. Pyrolysates were introduced into the ion source through an all glass heated inlet system, held at 300°C.²

FTIR spectra were recorded on a Bruker 113V FTIR spectrometer. Samples were quantitatively prepared as 13 mm KBr discs, and spectra normalized to 1.00 mg (resin) for presentation.

CP/MAS ¹³C NMR spectra were recorded on a Bruker CPX-100 NMR spectrometer, operating at a field strength of 2.35 T. Relevant operating parameters were as follows: spectral width = 10 kHz, contact time = 2 ms, pulse repetition rate = 2 sec, proton decoupling field = 56 kHz. Interrupted decoupling experiments used a 100 μs interruption to proton decoupling prior to acquisition.

RESULTS AND DISCUSSION

The results of pyrolysis-high resolution mass spectrometric analysis (Py-HRMS) of the resinite and bombicite samples characterized during the course of this study are illustrated in Figure 1. The close similarity of these data suggests that despite their physical dissimilarity, the chemical structures of these materials are very similar. In particular, these data indicate that species of molecular weight = 302, molecular formula = C₂₀H₃₀O₂ are a predominant subunit in both materials. This suggests that the macromolecular structures of these materials are based predominantly on diterpenoid monomers.

The results of spectroscopic analyses of resinite and bombicite are illustrated in Figures 2 (CP/MAS ¹³C NMR) and 3 (FTIR). The combination of normal CP/MAS ¹³C NMR, CP/MAS ¹³C NMR with interrupted proton decoupling (which reduces or eliminates signal due to protonated carbon) and FTIR, allows considerable

structural detail to be elucidated. Both ^{13}C NMR and FTIR data suggest that both the resinite and bomicite have predominantly aliphatic structures (which is consistent with the elemental composition of these samples - see Table 1). Also indicated is the presence of considerable amounts of oxygen containing functional groups, especially carboxylic acids. The absence of appreciable intensity in the 30 ppm region of the ^{13}C NMR spectra of these samples, and the lack of characteristic dominant IR absorption bands at 2926 cm^{-1} and 2853 cm^{-1} in the corresponding FTIR spectra, rule out the presence of polymethylene structures of significant chain length. Rather, the spectroscopic data suggest that their structures are based to a large extent on alicyclic structures. Strong IR absorbances at 1450 cm^{-1} and 1385 cm^{-1} in the FTIR spectra of both samples suggest a high degree of methyl substitution. Moreover, the partial disappearance of carbon resonances, at 15 ppm, 20 ppm, and 29 ppm in the proton decoupling interrupted ^{13}C NMR spectra, suggests that methyl groups exist in these samples in at least three structurally distinct environments.

^{13}C NMR resonances at 108 and 149 ppm, and moderately intense IR absorption at 887 cm^{-1} indicate the presence of exocyclic $\text{R}_2\text{C}=\text{CH}_2$ structures. Similarly, ^{13}C NMR resonances at 126 ppm and 139 ppm, which are absent and present respectively in the interrupted decoupling spectra, indicate that significant amounts of 1,1,2-trisubstituted C=C bonds are present in both samples. Significant carboxyl functionality in these materials is established by ^{13}C resonances at 180-190 ppm and strong FTIR absorbance at 1695 cm^{-1} .

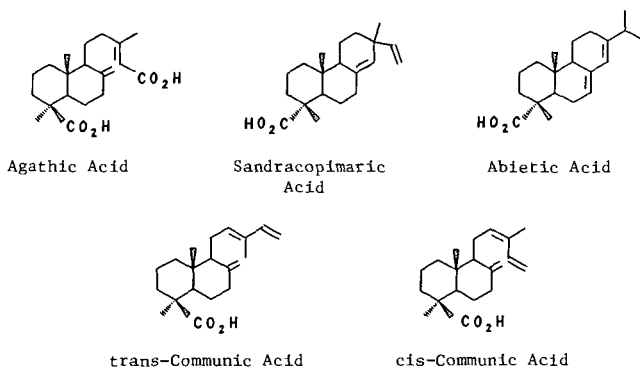
Other types of oxygen containing structures are also indicated by the spectroscopic data, although these differ between samples. The ^{13}C NMR resonance observed at 203 ppm (absent in the interrupted decoupling spectra) and IR absorbance at 1720 cm^{-1} in the spectra of the resinite sample, indicate that aldehydic compounds may contribute significantly to the structure of this material, and ^{13}C resonance at 72 ppm in the spectra of the bomicite sample indicates the incorporation of alcoholic or etheric structures into this material.

The results of analysis therefore suggest that these materials are based on cyclic diterpenoid units, which incorporate a significant degree of methyl substitution. The presence of an exocyclic C=C bond, and another, 1,1,2-trisubstituted, C=C bond is also indicated, as is the presence of carboxyl functionality. The inclusion of compounds of other structural composition, especially with respect to the nature of oxygen containing functional groups, is also indicated, but the structural units having the features described above appear to predominate, and are common to both samples.

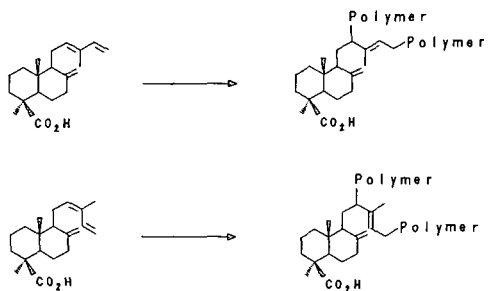
It has been noted that macroscopic resinite accumulations in VBC often occur in association with fossil logs of the genus *Agathis*. This association has not been specifically established for the samples used in this study, except, as already noted, that the bomicite sample characterized was found in intimate association with a large gymnosperm log. Nevertheless, this relationship has been established for a significant number of closely similar samples, and it is highly probable that the samples used in this study are derived from the bled resins of this species.

Modern *Agathis* resins were at one time of considerable commercial value, and as such, have been the subject of numerous investigations. Analysis of fresh bled resins of this species have demonstrated that the major components present are diterpenoid acids, specifically, those with the structures illustrated in Scheme 1. It has also been established that the solvent extracts of VBC resinites are rich in these acids, especially agathic acid, and their degradation products.³⁴

Based largely on the foregoing work, and more recently on spectroscopic evidence, previous workers have proposed structures for these resinites based on poly-agathic acid.³⁵ The mechanism proposed by these workers suggests that these resinites are formed by polymerization of (mainly) agathic acid with loss of the terminal C-15 carboxyl group. Such a polymeric structure would therefore be based predominantly on C_{10} monomers. The results of the analyses reported here however, clearly demonstrate the predominance of C_{20} products in both VBC resinite and bomicite, and hence preclude C_{10} monomers as a major structural subunit in these samples. The structure proposed by these authors,³⁵ however, very closely resembles those which can be drawn for the polymerization products of cis- and trans-communic acids, (as illustrated in Scheme 2), which are major components of fresh *Agathis* resins.⁶ These acids are known to readily polymerize on exposure to the atmosphere, and in some cases, poly-Communic acids have been shown to constitute a significant fraction of fresh and recent resins.⁷



Scheme 1.



Scheme 2.

CONCLUSIONS

The results of this study of VBC resinites suggest that these materials are not based on poly-agathic acid structures as has been previously proposed. The data obtained indicate the predominance of structural subunits of molecular formula $C_{20}H_{30}O_2$, which are consistent with a poly-communic acid based polymeric resinite structure. Other materials may be incorporated into the polymeric structure to a lesser degree, and may also be physically occluded within it.

ACKNOWLEDGMENTS

This work was performed under the auspices of the Office of Basic Energy Sciences, Division of Chemical Sciences, U.S. Department of Energy, under contract number W-31-109-ENG-38. The authors would like to thank Dr. T. V. Verheyen, Coal Corp. of Victoria, for supplying the samples used in this study.

REFERENCES

1. Based in part on: Anderson, K.B. (1989), PhD Thesis, University of Melbourne.
2. Winans, R.E., McBeth, R.L. and Neill, P.H. (1988), ACS Division of Fuel Chem. Preprints, 33(3): 85-90.
3. Brooks, J.D. and Steven J.R. (1967), Fuel, 46: 13-18.
4. Allan, J. (1975), PhD Thesis, University of Newcastle-upon-Tyne.
5. Wilson, M.A., Collin, P.J., Vassallo, A.M. and Russell, N.J. (1986), Org. Geochem. 7(2): 161-168.
6. Thomas, B.R. (1969), In: "Organic geochemistry - methods and results", G. Eglinton and M.T.J. Murphy (eds), Springer-Verlag, N.Y. pp 599-618.
7. Carman, R.M., Cowley, D.E. and Marty, R.A. (1970), Aust. J. Chem., 23: 1655-1665.

TABLE 1.

	Elemental Composition (wt%)					Molecular Formula (based on C_{20})
	C	H	N	S	O	
Resinite	79.78	10.19	-	0.03	10.00	$C_{20}H_{30.6}O_{1.8}$
Bombicite	75.17	9.47	-	0.06	15.31	$C_{20}H_{30.2}O_{3.1}$
poly-Communic Acid	79.5	9.9	-	-	10.6	$C_{20}H_{30}O_2$

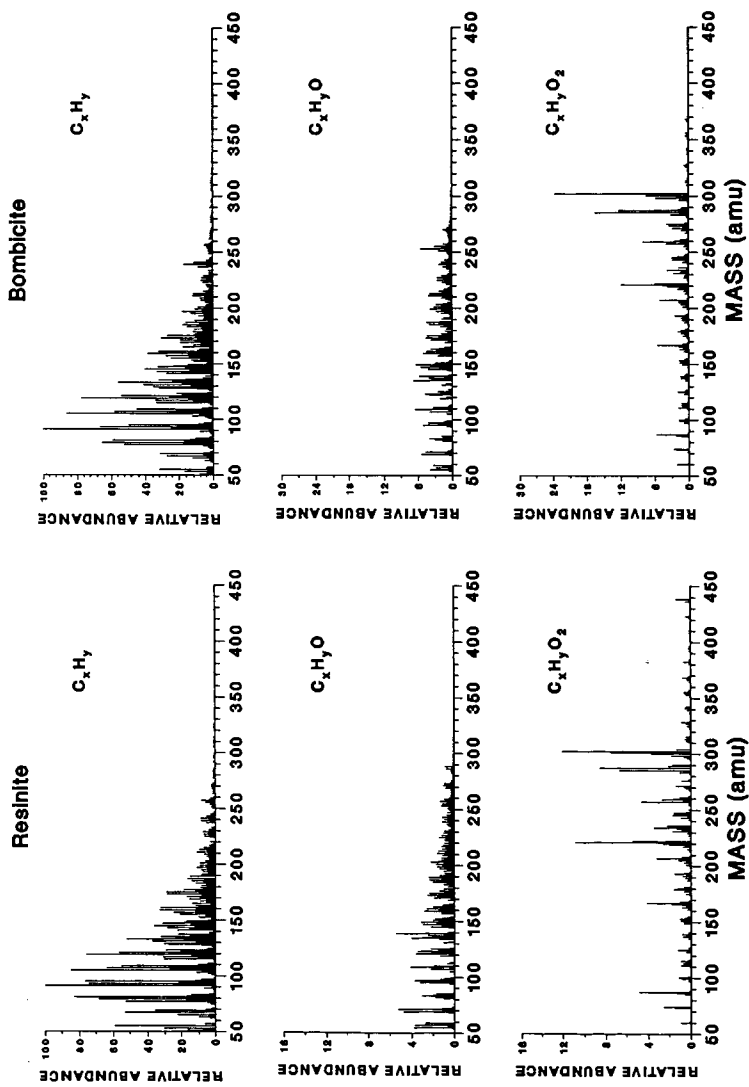


Figure 1. Mass spectra of selected ion classes obtained by Py-HRMS of VBC resinite and bombicite (averaged over 50 scans).

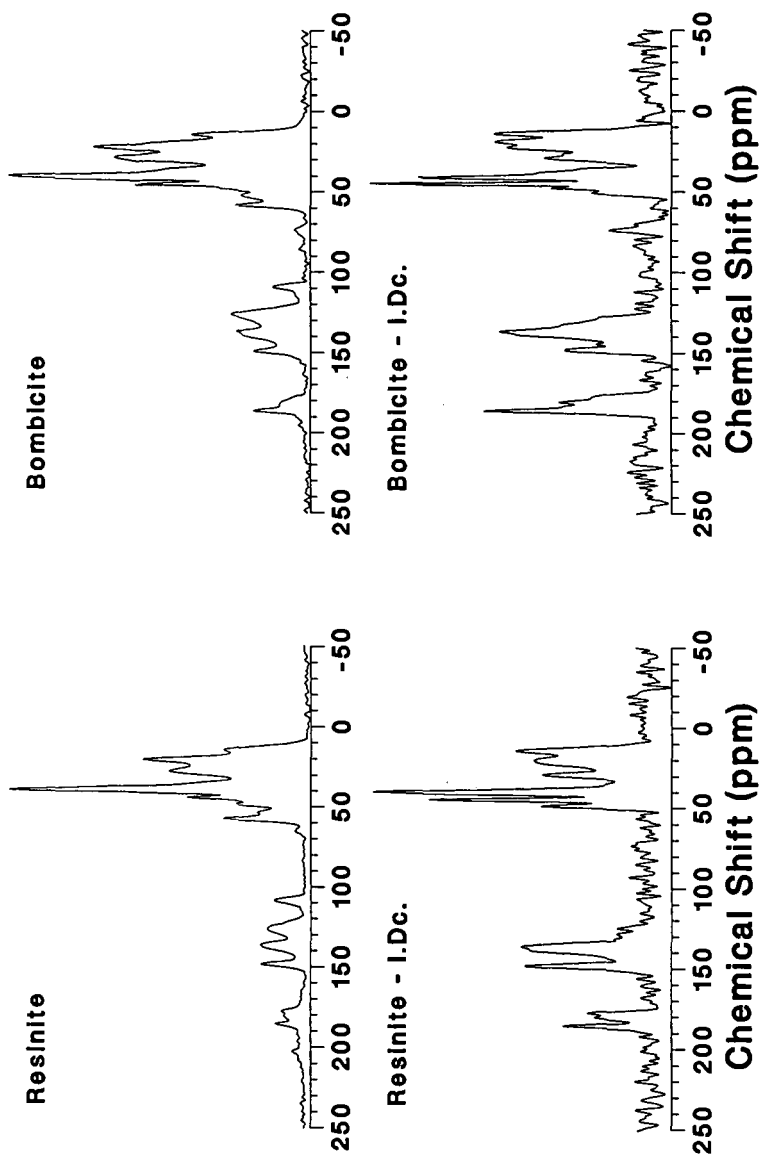


Figure 2. CP/MAS ^{13}C NMR spectra, and Interrupted Proton Decoupling (I.D.c.) CP/MAS ^{13}C NMR spectra of VBC resinite and bombicite.

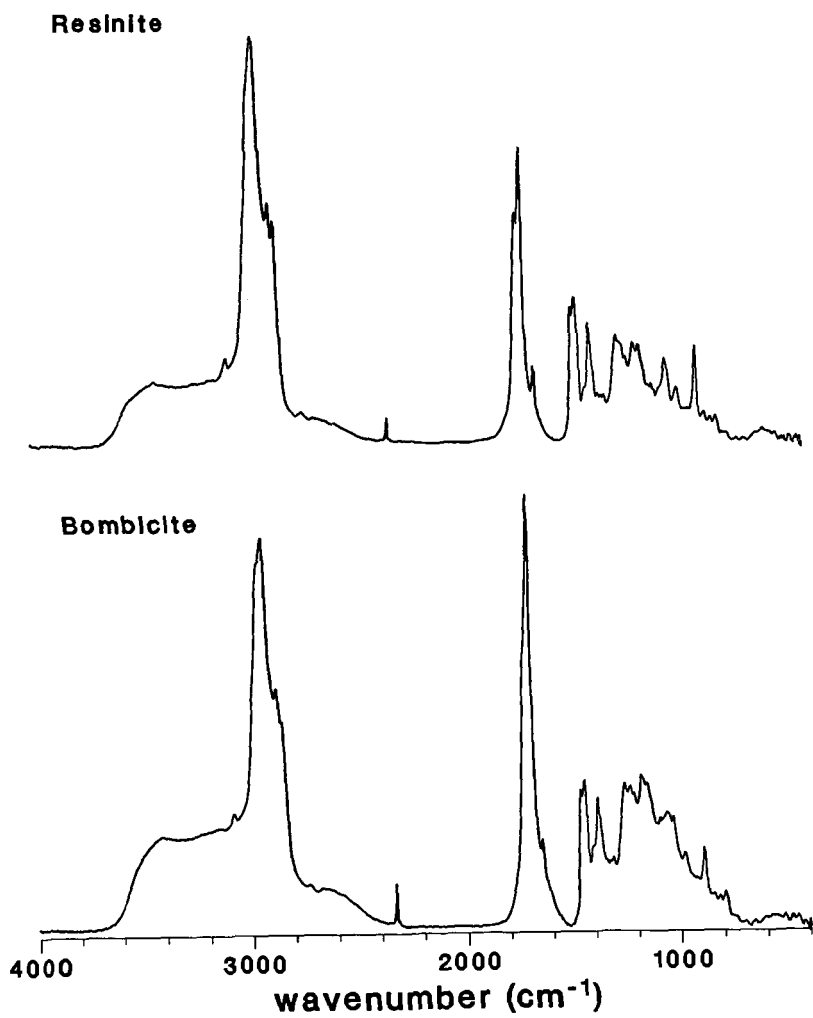


Figure 3. FTIR spectra of VBC resinite and bombicite.

SWELLING OF COAL EXTRACTS

T.K. Green, J.M. Chamberlin, and L. Lopez-Froedge
Department of Chemistry
Western Kentucky University
Bowling Green, KY 42101

INTRODUCTION

Coals are considered macromolecular solids. (1) Although they are not polymers in the sense that they possess a repeating unit, they do possess several fundamental properties typical of synthetic crosslinked polymers. (2) One of these properties is the ability of coals to swell in organic solvents without dissolving.

In recent years, there has been a rapid growth in the number of publications that deal with the solvent swelling of coal. Much of this effort has been directed toward the application of modern polymer and network theories to coal, with the purpose of better understanding their network structures. One of the most fundamental properties of a network structure is \bar{M}_c , the average molecular weight between crosslinks. Consequently, several research groups have attempted to estimate \bar{M}_c 's for coal from solvent swelling data and the Flory-Rehner equation. (3-8) The equation incorporates both the Flory-Huggins theory of polymer solutions and the Gaussian elastic network theory. An important parameter embodied in the Flory-Huggins theory is the interaction parameter, χ . χ is a thermodynamic parameter describing the energetics of the polymer-solvent interaction. A reliable evaluation of χ is essential to an estimation of \bar{M}_c for crosslinked networks using the Flory-Rehner equation. Very few reliable methods have been developed to evaluate χ for coal-solvent systems. It is the purpose of this research to develop a reliable method for its evaluation.

Approach. One of the most common techniques for determining χ parameters for polymer-solvent systems is the vapor sorption method. (9) In this approach, the uncrosslinked polymer is exposed to solvent vapor of known pressure, p . The polymer absorbs solvent until equilibrium is established. χ is related to p and v_2 , the volume fraction of polymer at equilibrium, by

$$\chi = \frac{\ln [(p/p_0)/(1-v_2)]}{v_2^2} - v_2 \quad 1)$$

Measurement of p as a function of v_2 can be used with Equation 1 to obtain values for χ over a wide range of concentrations.

It is important to recognize that Equation 1 applies to polymers that are not crosslinked. Most vapor sorption studies on coal have been conducted on the crosslinked, or insoluble portion of coals. Under this condition, simultaneous evaluation of χ and \bar{M}_c must be made. Two groups of researchers have adopted this approach. (7,8) We have adopted an alternative approach by conducting vapor sorption studies on the uncrosslinked portion of the coal. χ parameters can thus be directly calculated from the pressure-sorption data using Equation 1.

The uncrosslinked portion of the coal is obtained by Soxhlet-extraction of the coal with pyridine. Pyridine is a particularly good solvent for coals, and it is thought to remove a majority of the uncrosslinked molecules from the coal matrix. There is evidence that the pyridine-soluble portion is representative of the larger, crosslinked portion, although this aspect remains controversial.

EXPERIMENTAL

Sample Preparation. Dry Illinois No. 6 (Herrin seam, -60 mesh) was used in the sorption studies. Analysis Found: C, 74.37; H, 4.83; N, 1.76; S, 1.76; O (by difference), 8.74; Ash, 8.33 (duplicate). Approximately 10 g of the sample was exhaustively Soxhlet-extracted with pyridine. Extractability was 18.7% (wt.). The pyridine solution was then filtered through a 0.4 μ m filter. Most of the pyridine was removed by rotovaporization under reduced pressure at 70-80°C. Approximately 200 mL of a methanol/water (80/20 vol) mixture and 2 mL of conc. HCl were added to the flask and the mixture was stirred under nitrogen for two days. The solid extract was then filtered and dried under vacuum at 105°C for 24 hours. Analysis Found: C, 82.97; H, 5.87; N, 1.80 (duplicate).

O-Methylation Procedure. The extract was O-methylated according to a method described earlier by Liotta (10) using tetrabutylammonium hydroxide and methyl iodide.

Sorption Experiments. Sorption experiments were carried out using a Cahn 1000 recording balance, with an accuracy of ± 0.03 mg. The balance and its accessories are shown in Figure 1. The instrument is equipped with an MKS Baratron pressure transducer (0-100 torr, 0.15% accuracy) with a digital readout for pressure measurements.

Prior to conducting the sorption experiment, the coal extract (200 mg) was first placed in a Wig-L-Bug capsule and ground for 1 minute under nitrogen. This grinding effectively reduces the extract to a fine powder, which is then used for the sorption experiment. Approximately 50-70 mg of the extract was then placed on the sample pan and the hangdown tube was replaced. The sample was maintained at 30.00 ± 0.02 °C by means of a constant temperature bath which surrounded the hangdown tube.

In a typical experiment, benzene vapor was admitted into the evacuated balance chamber by means of stopcock D. After achieving the desired pressure, stopcock D was closed. The maximum uncertainty in p/p₀ during the course of any one experiment was ± 0.008 units. Equilibrium was judged to be established when there was less than a 1 percent change in weight over a 12 hour period.

RESULTS

Characterization of the Pyridine-Extract. Pyridine is known to cling to coals. The extract was therefore stirred with a methanol/water/HCl mixture for two days as suggested by Buchanan. (11) Elemental analysis of the extract revealed 1.80% N. The original coal contained 1.92% N (daf) so it is apparent that the methanol/water/HCl treatment followed by drying successfully removed pyridine from the extract.

Synthesis and Characterization of O-Methylated Extract. The O-alkylation of coals has been discussed by Liotta *et al.* (10) Alkylation occurs when tetrabutylammonium hydroxide is used to promote the reaction of the alkyl iodide with the coal in tetrahydrofuran. The alkylation reaction occurs primarily on acidic oxygen functionalities such as phenolic hydroxyl and carboxylic acid groups, as shown below.



The hydrogen to carbon ratios of the extract and O-alkylated extract established that 4 hydroxyl groups per 100 carbon atoms were alkylated. FT-IR and ^{13}C NMR analysis confirmed that O-methylation had occurred.

Sorption Experiments. The extracts were exposed to benzene vapor at several relative vapor pressures (p/p_0). Two types of sorption experiments were conducted. Experiments in which the benzene vapor pressure is raised from zero to a higher value are termed integral sorptions. Sorption experiments starting with the extract and vapor in equilibrium at a finite, non-zero pressure, and proceeding to a higher pressure, are termed incremental sorptions.

Figures 2 and 3 show the sorption curves of mass uptake versus time for the extract and O-methylated extract. Three different experiments are shown in each figure; a single integral sorption and two subsequent incremental sorptions. Both extracts required 30 to 150 hours to reach equilibrium, depending on the particular experiment.

Sorption-Desorption Isotherms. Sorption-desorption isotherms for the extracts are presented in Figures 4 and 5, where the relative vapor pressure of benzene (p/p_0) is plotted against the cumulative equilibrium uptake of benzene. Both isotherms are characterized by strong hysteresis (non-reversible sorption behavior). For both extracts, a considerable amount of benzene cannot be desorbed under vacuum (~ 0.01 torr). However, the benzene could be completely removed from the O-methylated extract by heating to 105°C under vacuum. Thus benzene is not irreversibly bound to the O-methylated extract. Once the benzene was driven off, the sorption curve could be reproduced. We did not apply this procedure to the extract, but we expect it to behave similarly.

DISCUSSION

The sorption of benzene by the extract and the O-methylated extract is characterized by a rapid, initial uptake followed by a slow approach to equilibrium. Such sorption behavior is very similar to that of glassy polymers. Thus we have chosen to interpret the sorption curves shown in Figures 2 and 3 in terms of the Berens-Hopfenberg model developed for sorption of organic vapors into glassy polymers.⁽¹²⁾

The Berens-Hopfenberg Model. The Berens and Hopfenberg model considers the sorption process in glassy polymers as a linear superposition of independent contributions of a rapid Fickian diffusion into pre-existing holes or vacancies (adsorption) and a slower relaxation of the polymeric network (swelling). The total amount of sorption per unit weight of polymer may be expressed as

$$M_t = M_{t,F} + M_{t,R} \quad 2)$$

where $M_{t,F}$ and $M_{t,R}$ are the contributions of the Fickian and relaxation processes, respectively.

The relaxation or swelling process is assumed to be first order in the concentration difference which drives the relaxation and is expressed as

$$M_{t,R} = M_{\infty,R} [1 - \exp(-kt)] \quad 3)$$

where k is the relaxation rate constant and $M_{\infty,R}$ is the ultimate amount of sorption due to relaxation. The relaxation process is interpreted as a structural reordering

or swelling of the polymeric network. It is the swelling term which is of crucial importance to our study.

Interpretation of Sorption Curves. The slow asymptotic approach to equilibrium exhibited by the extract and O-methylated extract, as shown in Figures 2 and 3, strongly suggest that this process might correspond to the first-order relaxation or swelling process described in the Berens-Hopfenberg model, and that the initial rapid uptake may correspond to hole filling and/or adsorption onto surfaces. To test whether this slow process follows first-order behavior, we have plotted the natural log of the difference between the equilibrium sorption value, M_{∞} , and the sorption value at any time, M_t , against time. The results are shown in Figures 6 and 7. Note that a substantial portion of each curve is linear or nearly linear at long times, indicating a first-order process. This is particularly evident for the incremental sorption where linearity is observed over a 50 to 60 hour period. At short times, the curves clearly deviate from linearity, suggesting that other processes are dominating.

We suggest that the rapid process corresponds to hole-filling and/or adsorption onto external surfaces, and that the slow process, which follows first-order behavior, corresponds to swelling of the coal extract. Extrapolation of the linear portion of the curves shown in Figures 6 and 7 to time zero should yield the total uptake of benzene attributed to swelling. The results of this analysis are summarized in Table I, where the total benzene uptake, M_{∞} , and the uptake attributed to the hole-filling/adsorption and the swelling processes, M_{ads} and M_{swell} , are shown.

If this interpretation of the sorption process is correct, it indicates that when the benzene pressure is raised from zero to an activity of 0.22, the dominant process is hole-filling and/or adsorption, with only a relatively minor contribution from actual swelling. However, in subsequent incremental sorptions, the swelling process is clearly dominant. These results are similar to those of Berens and Hopfenberg in their studies on glassy polyvinylchloride.(12) According to their interpretation, the polymer is initially penetrant-free in an integral sorption experiment, and the hole-filling process therefore dominates. Incremental sorptions, however, proceed with polymer in which most of the sorption holes are pre-saturated. The relative contribution of swelling is therefore larger in these experiments.

The data in Table I also indicate that the O-methylated extract swells roughly one and a half times the extract. These results are consistent with those of Larsen et al.(6), who observed that O-methylated coals swell substantially more than underivatized coals.

The swelling data in Table I can be used to calculate χ parameters for the extract and O-methylated extract using Equation (1). A knowledge of the densities of the extracts is required to convert the masses to volume fractions. We have assumed densities of 1.4 and 1.3 g/mL for the extract and O-methylated extract, respectively. These are the helium densities (dmf basis) for the Illinois No. 6 coal and its O-methylated derivative as determined by Liotta.(10) A density of 0.88 g/mL for benzene was used. Additivity of volumes was also assumed. The results of these calculations are shown in Table II.

The χ parameters are observed to be positive and independent of vapor pressure (or concentration). According to Flory-Huggins theory, polymer-solvent systems with χ parameters above 0.5 should show only limited solubility.(2) Thus the extracts

should not dissolve in liquid benzene but should show limited swelling. Liquid volumetric swelling measurements verify this expectation. The bulk of both extracts remain insoluble in liquid benzene, although some dissolution occurs. Moreover, both extracts exhibit limiting swelling, with the O-methylated extract swelling more than the extract, consistent with the gravimetric data presented in Table I. χ parameters were calculated from the volumetric data assuming a p/p_0 of 1.0, and are shown in Table II. The volumetric method yields χ parameters consistent with those calculated from the gravimetric data.

Finally, a calculation of the solubility parameter of the extracts can be made using the equation

$$\delta_e = \left(\frac{(\chi - 0.30)RT}{V} \right)^{1/2} + \delta_s \quad (4)$$

where δ_e and δ_s are the solubility parameters of the extract and solvent, respectively, and V is the molar volume of benzene (89 mL/mol). Using a δ_s of 9.2 Hildebrands for benzene and a χ of 1.5 for the extract, δ_e of 12.0 Hildebrands is calculated for the extract. The same calculation using a χ of 1.1 for the O-methylated extract yields a δ_e of 11.5 Hildebrands. Van Krevelen has estimated solubility parameters of coals using a group contribution method and has calculated values ranging from 10.6 to 15.2 Hildebrands.(13) Thus the solubility parameters calculated for the extracts fall within the accepted range of solubility parameters for coals.

CONCLUSIONS

The sorption of benzene by an extract and O-methylated extract of an Illinois No. 6 coal is characterized by an initial, rapid uptake of solvent vapor, followed by a slow asymptotic approach to equilibrium. The slow process appears to follow first-order behavior. We have suggested that this slow, first-order process corresponds to the swelling of the extract. There are several lines of indirect evidence to suggest that this interpretation is correct.

- (1) The results show that the O-methylated extract swells more than the underivatized extract, consistent with other swelling studies.
- (2) The χ parameters calculated for the benzene-extract systems are consistent with the fact that the bulk of these extracts remain insoluble in liquid benzene. The extracts, however, exhibit limited swelling. The χ parameters calculated from the volumetric data are consistent with those derived from the gravimetric data.
- (3) The solubility parameters of the extracts calculated from the χ parameters fall within the accepted range of solubility parameters for coals.

ACKNOWLEDGEMENT

This work was supported by a grant from the U.S. Department of Energy, Grant No. DE-FG22-88PC88924, and the Research Corporation.

REFERENCES

1. T. Green, J. Kovac, D. Brenner, and J.W. Larsen in "Coal Structure," R. A. Meyer, Ed., Academic Press, New York, N.Y., p. 199.
2. L.R.G. Treloar, "The Physics of Rubber of Elasticity," Clarendon Press, Oxford, 1975, pp. 128-139.
3. Y. Sanada and H. Honda, Fuel, 46, 451 (1967).
4. N.Y. Kirov, J.M. O'Shea, and G.D. Sergeant, Fuel, 47, 415 (1967).
5. N.A. Peppas and M.L. Lucht, "Investigations of the Crosslinked Macromolecular Nature of Bituminous Coals," Final Report, DOE Contract No. DE-F622-78E, 12279 (1980).
6. J.W. Larsen, T.K. Green, J. Kovac, J. Org. Chem., 50, 4729 (1985).
7. S.T. Hsieh and J.L. Duda, Fuel, 66, 170 (1987).
8. J.R. Nelson, O.P. Mahajan, and P.L. Walker, Fuel, 58, 831 (1980).
9. D.C. Bonner, J. Macrol. Sci. - Revs. Macrol. Chem. C13(2), 263-319 (1975).
10. R. Liotta, K. Rose, E. Hippo, J. Org. Chem., 1981, 50, 277-283.
11. D.H. Buchanan, K. Osborne, L.C. Warfel, M. Wampang, D. Lucas, Energy & Fuel, 1988, 2, 113-170.
12. A.R. Berens and H.B. Hopfenberg, Polymer, 1978, 5, 489.
13. D.W. Van Krevelen, Fuel, 1966, 45, 229.

TABLE I

Benzene Sorption Data for Extract and O-Methylated
Extract of Illinois No. 6 Coal at 30°C

Pressure Interval <u>p/p₀</u>	Extract (mg/g)			O-Methylated (mg/g)		
	<u>M_a</u>	<u>M_{ads}</u>	<u>M_{swell}</u>	<u>M_a</u>	<u>M_{ads}</u>	<u>M_{swell}</u>
0 - 0.22	76	64	12	78	56	22
0.22-0.44	38	17	21	32	7	25
0.44-0.66	<u>34</u>	<u>12</u>	<u>22</u>	<u>50^a</u>	<u>6</u>	<u>44</u>
Total:	148	93	55	160	69	91

^a p/p₀ = 0.44 - 0.67

TABLE II

Volume Fractions of Solvent and χ Parameters
for the Extract and O-Methylated Extract of
Illinois No. 6 Coal and Benzene

p/p_0	Extract		O-Methylated	
	v_1	χ	v_1	χ
0.22	0.019	1.5	0.031	1.1
0.44	0.050	1.4	0.065	1.1
0.66	0.080	1.4	0.12	1.1 ^a
1.0 ^b	0.12	1.6	0.25	1.1

^a $p/p_0 = 0.67$

^b v_1 determined from direct volumetric swelling
method using liquid benzene.

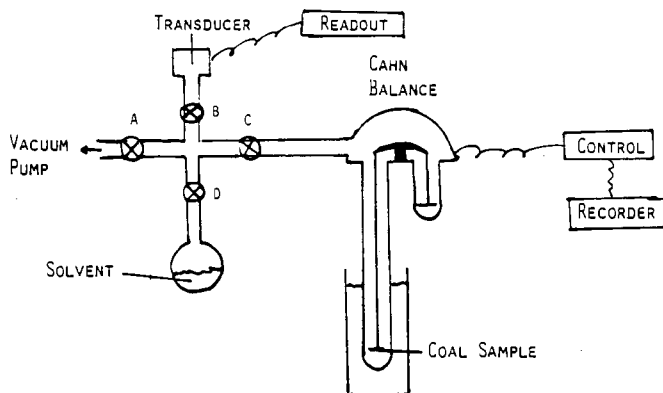


Figure 1. Sorption Apparatus

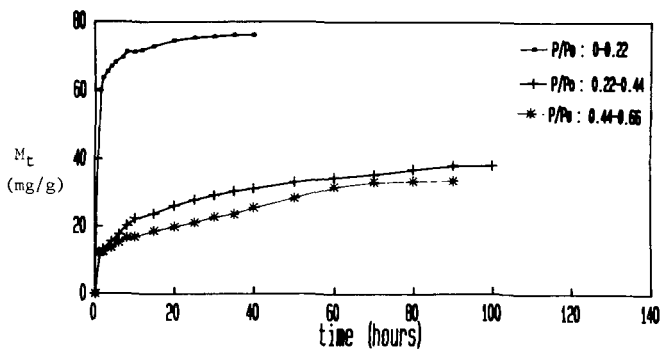


Figure 2. Sorption of Benzene by the Pyridine-Extract of Illinois No. 6 Coal at 30°C.

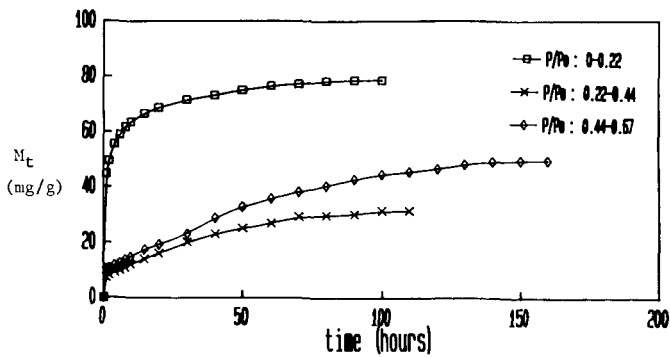


Figure 3. Sorption of Benzene by the O-methylated Extract of Illinois No. 6 Coal at 30°C.

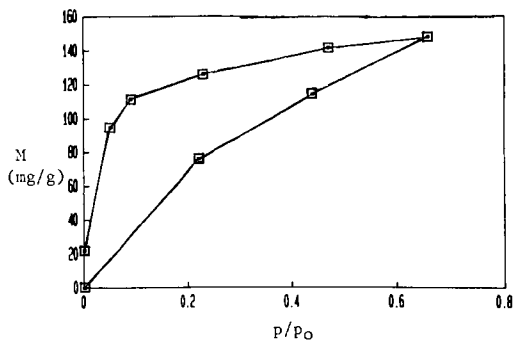


Figure 4. Sorption-desorption Isotherm for the Extract of Illinois No. 6 Coal and Benzene at 30°C.

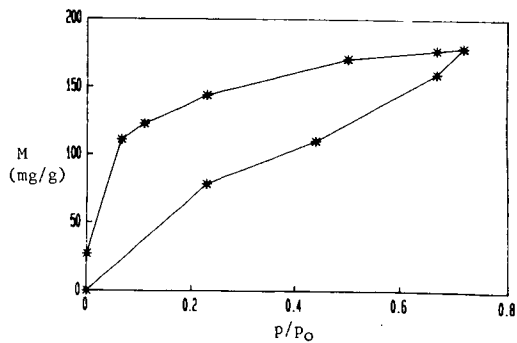


Figure 5. Sorption-desorption Isotherm for the O-methylated Extract of Illinois No. 6 Coal and Benzene at 30°C.

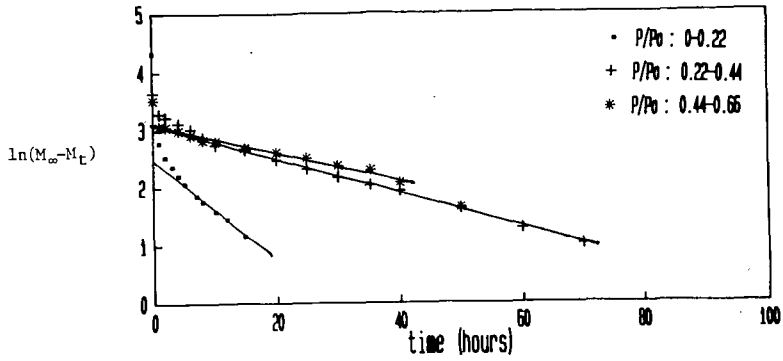


Figure 6. Plot of $\ln(M_\infty - M_t)$ versus Time for Extract-Benzene System.

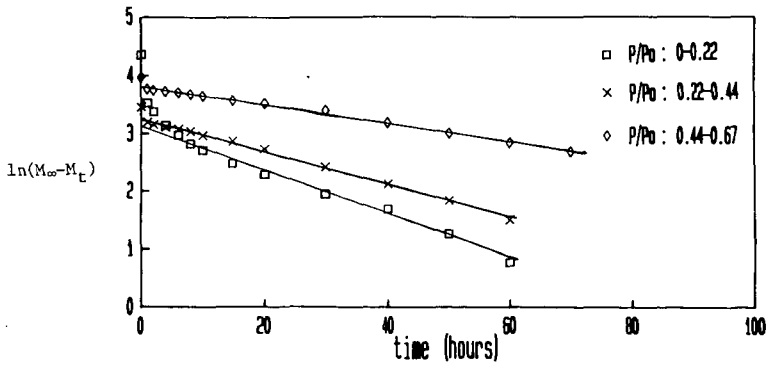


Figure 7. Plot of $\ln(M_\infty - M_t)$ versus Time for O-methylated Extract-Benzene System.